LUND UNIVERSITY

Magnetic losses in composite materials

Ramprecht, Jörgen; Sjöberg, Daniel

2008

Magnetic losses in composite materials

Jörgen Ramprecht and Daniel Sjöberg

Electromagnetic Theory
Department of Electrical and Information Technology
Lund University
Sweden
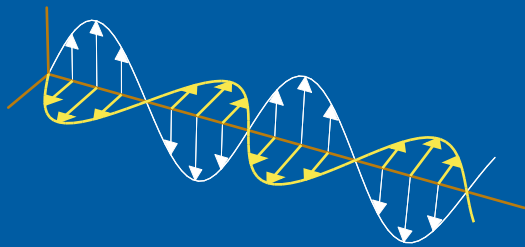
Jörgen Ramprecht
jorgen.ramprecht@ee.kth.se

Division of Electromagnetic Engineering
School of Electrical Engineering
Royal Institute of Technology
Sweden

Daniel Sjöberg
daniel.sjoberg@eit.lth.se

Department of Electrical and Information Technology
Electromagnetic Theory
P.O. Box 118
SE-221 00 Lund
Sweden

Abstract

We discuss some of the problems involved in homogenization of a composite material built from ferromagnetic inclusions in a nonmagnetic background material. The small signal permeability for a ferromagnetic spherical particle is combined with a homogenization formula to give an effective permeability for the composite material. The composite material inherits the gyrotropic structure and resonant behavior of the single particle. The resonance frequency of the composite material is found to be independent of the volume fraction, unlike dielectric composite materials. The magnetic losses are described by a magnetic conductivity which can be made independent of frequency and proportional to the volume fraction by choosing a certain bias. Finally, some concerns regarding particles of small size, *i.e.*, nanoparticles, are treated and the possibility of exciting exchange modes are discussed. These exchange modes may be an interesting way to increase losses in composite materials.

1 Introduction

Due to the possibility of manufacturing ferromagnetic fine particles of very small dimensions with well-defined characteristics and narrow distribution of particle size [28], research on ferromagnetic nanoparticles has been of great interest over the past years. Since ferromagnetic media interact with magnetic fields, ferromagnetic nanoparticles are capable of being used in a wide variety of fields such as magnetic recording media, ferrofluids [24], medical applications [13] and microwave composite materials for absorption of electromagnetic energy [5].

In this paper our attention is mainly directed towards absorption of electromagnetic energy and the losses associated with ferromagnetic nanoparticles. The overall aim is to study if a composite material with ferromagnetic nanoparticles can be constructed with substantial magnetic losses. The geometry proposed is depicted in Figure 1.

A review of losses in magnetic materials can be found in [11] and the main loss mechanisms mentioned are hysteresis, domain wall motion, eddy currents, and ferromagnetic resonance (FMR). However, at microwave frequencies we only have to consider the last two since the others are relatively low frequency phenomena. For nanoparticles with diameters below $1\,\mu$m the exchange interactions have to be taken into account, resulting in the possibility of excitation of exchange modes [1, 2, 14]. The existence of exchange modes is typically manifested by several particle size dependent resonance peaks in the absorption spectra [21, 29]. This phenomenon is sometimes referred to as spin wave resonance (SWR) [16] and may lead to an increase of the magnetic losses. Therefore, ferromagnetic nanoparticles have the potential of being a good candidate as a component in a composite material designed for absorbing electromagnetic energy. In radar absorbing applications, the main reason for using composite material with ferromagnetic inclusions is to reduce the effect due to the electric conductivity, resulting in the losses being almost purely magnetic. Magnetic radar absorbing materials (RAM) can be made very thin with an improved bandwidth compared to electric RAMs [17, p. 334].
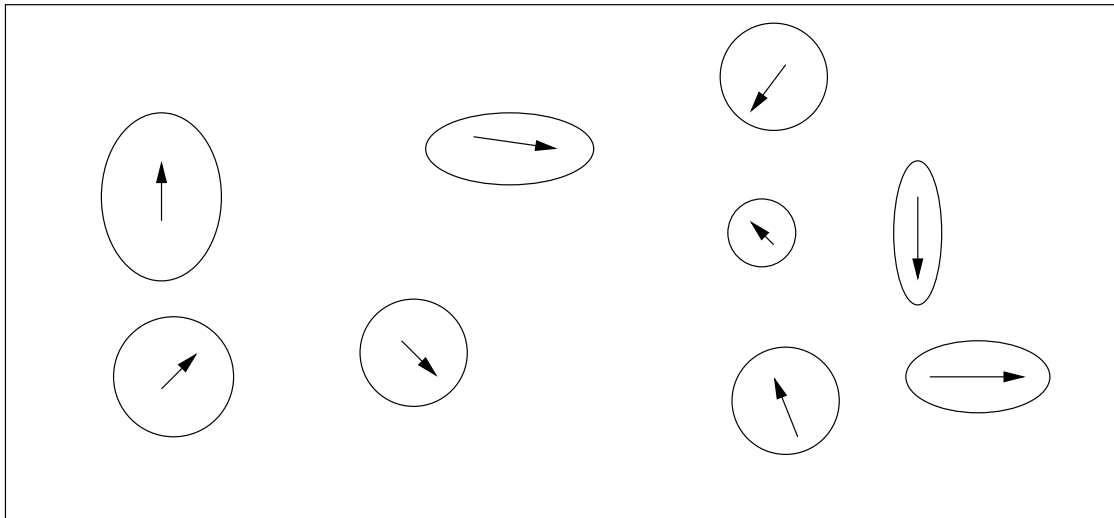
Figure 1: Geometry of the composite material. Each inclusion is a single-domain particle, roughly of dimensions 100 nm or less. Due to the small size, each particle is uniformly magnetized with magnetization $\boldsymbol{M}_n$. The amplitude is the same for all particles, $|\boldsymbol{M}_n| = |\boldsymbol{M}_{n'}| = M_\mathrm{S}$ where M_S is the saturation magnetization of the ferromagnetic material, but the direction of the magnetization may be different in different particles.

When modeling composite materials, homogenization methods are often applied. The composite is then essentially treated as a homogenous material with effective material parameters. Such a homogenization procedure is motivated for materials where the typical length scale of the inhomogeneities in the microstructure are small compared to the wavelength. At microwave frequencies, nanoparticles obviously meet this criterion. An exhaustive presentation on modern homogenization theory can be found in [23].

In the present work we analyze a composite material consisting of ferromagnetic spherical nanoparticles embedded in a background material. The magnetic properties of a ferromagnetic spherical particle biased by an external magnetic field are modelled by the Landau-Lifshitz-Gilbert (LLG) equation, resulting in a gyrotropic small signal permeability with a resonance behavior. The effects of eddy currents and exchange modes in a spherical particle are then investigated. It is found that eddy currents at microwave frequencies can be neglected in nanoparticles and that an applied time harmonic magnetic field can excite exchange modes. However, it seems that surface anisotropy, *i.e.*, pinning of the spins at the surface, plays a crucial role when analyzing the exchange modes and their resonance frequencies. This is also pointed out in [2]. Further, the permeability of the single particle is then combined with a homogenization formula to obtain an effective permeability for the composite material. It is found that the material remains gyrotropic and that the resonance frequency of the single particle is preserved. We also show that a magnetic conductivity can be identified, and that it is independent of frequency for a

certain bias condition. Finally, bounds for the complex effective permeability of the composite material are discussed.

2 Equation of motion

The time evolution of the magnetization vector is described by the Landau-Lifshitz-Gilbert equation [19]

$$\frac{\partial \boldsymbol{M}}{\partial t} = -\gamma \mu_0 \boldsymbol{M} \times \boldsymbol{H}_{\text{eff}} + \alpha \frac{\boldsymbol{M}}{M_{\text{S}}} \times \frac{\partial \boldsymbol{M}}{\partial t} \tag{2.1}$$

The constant $\gamma = ge/2m_{\text{e}} = 1.759 \cdot 10^{11}\,\text{C/kg}$ is the gyromagnetic ratio for the material, and α is a dimensionless constant typically at most in the order of 0.1. However, for bulk materials values as large as 0.4 [31] and 0.92 [32] can be found, and for single domain particles values in the range 0.2–0.6 are reported [28]. It is immediately clear from this equation that the magnitude of the magnetization is preserved: since the right hand side is orthogonal to $\boldsymbol{M}$ due to the vector products, we have

$$\boldsymbol{M} \cdot \frac{\partial \boldsymbol{M}}{\partial t} = \frac{\partial}{\partial t} \frac{|\boldsymbol{M}|^2}{2} = 0 \quad \Rightarrow \quad |\boldsymbol{M}| = M_{\text{S}} \tag{2.2}$$

where the constant M_{S} is the saturation magnetization. Thus, the magnetization can only change its direction, not its magnitude.

The effective field $\boldsymbol{H}_{\text{eff}}$ is the local field producing the torque on the magnetic moment. This has several contributions, not all of which are easy to understand [10]:

$$\boldsymbol{H}_{\text{eff}} = \boldsymbol{H} + \boldsymbol{H}_{\text{an}} + \boldsymbol{H}_{\text{ex}} + \boldsymbol{H}_{\text{me}} \tag{2.3}$$

The field $\boldsymbol{H}$ is the classical magnetic field, which is the one appearing in Maxwell's equations, whereas the remaining fields are of microscopic (quantum mechanical) origin. The magnetocrystalline anisotropy field $\boldsymbol{H}_{\text{an}}$ is due to the atomic lattice and can generally be calculated from the anisotropy energy U_{an} as $\mu_0 \boldsymbol{H}_{\text{an}} = -\partial U_{\text{an}}/\partial \boldsymbol{M}$. To first order, the anisotropy can be modeled with a symmetric tensor $\mathbf{N}_{\text{c}}$ such that $U_{\text{an}} = \frac{\mu_0}{2}\boldsymbol{M} \cdot \mathbf{N}_{\text{c}}\boldsymbol{M}$ and $\boldsymbol{H}_{\text{an}} = -\mathbf{N}_{\text{c}}\boldsymbol{M}$ [4]. For a uniaxial crystal with axis $\hat{\boldsymbol{a}}$, we have $\mathbf{N}_{\text{c}} = N_{\text{c}}\hat{\boldsymbol{a}}\hat{\boldsymbol{a}}$. The case $N_{\text{c}} < 0$ is termed *easy axis*, and the case $N_{\text{c}} > 0$ is termed *easy plane*. The exchange field $\boldsymbol{H}_{\text{ex}}$ is due to the nonuniformity of the magnetization and can be modeled as $\boldsymbol{H}_{\text{ex}} = \lambda_{\text{ex}}\nabla^2 \boldsymbol{M}$. The combination of these two contributions is usually responsible for setting up the magnetic domains. Finally, the magnetoelastic field $\boldsymbol{H}_{\text{me}}$ models the possible influence of mechanical strain on the magnetization. For typical values of the parameters, see Table 1.

It is a delicate matter to determine which of these fields to include in or exclude from the model. In this document, we do not consider the magnetoelastic field $\boldsymbol{H}_{\text{me}}$, and focus on the purely electromagnetic properties.

3 Small signal solution

A small signal analysis was performed in [25], which is briefly repeated and augmented here. We assume the classical magnetic field, which is the one we can

Material	T_C	$\mu_0 M_S$	N_c	l_{ex}	f_S
Unit	[K]	[T]		[nm]	[GHz]
Fe	1044	2.16	-0.026	2.8	61
Co	1398	1.82	-0.038	3.4	51
Ni	627	0.62	0.037	9.9	17
Permalloy	720	1.0	0	5.7	28
CrO_2		0.5	-0.22	3.2	14
$SmCo_5$	993	1.05	-39	7.4	29

Table 1: Main properties of ferromagnetic materials, data taken from [7, p. 137]. T_C is the Curie temperature of the material, M_S is the saturation magnetization, N_c is the principal value of the crystalline anisotropy tensor $\mathbf{N}_c$ (computed as $N_c = -2K_1/(\mu_0 M_S^2)$ due to [7, eq. (2.12), p. 41], where K_1 is the uniaxial magneto-crystalline anisotropy constant as given in [7, p. 137]), l_{ex} is the exchange length of the material (computed as $l_{ex} = \sqrt{\lambda_{ex}} = \sqrt{2A/(\mu_0 M_S^2)}$, where A is the exchange constant as given in [7, p. 137]), and $f_S = \gamma \mu_0 M_S/2\pi = \omega_S/2\pi$ is the intrinsic precession frequency.

control, has one static bias part and one signal part (time convention $\mathrm{e}^{-\mathrm{i}\omega t}$), with the resulting splitting of the magnetization and effective field,

$$\boldsymbol{H} = \boldsymbol{H}_0 + \boldsymbol{H}_1 \mathrm{e}^{-\mathrm{i}\omega t}, \quad \boldsymbol{M} = \boldsymbol{M}_0 + \boldsymbol{M}_1 \mathrm{e}^{-\mathrm{i}\omega t}, \quad \boldsymbol{H}_{\mathrm{eff}} = \boldsymbol{H}_{\mathrm{eff},0} + \boldsymbol{H}_{\mathrm{eff},1} \mathrm{e}^{-\mathrm{i}\omega t} \quad (3.1)$$

where index 0 corresponds to fields constant in time, and time harmonic fields are indexed by 1. In general, all sorts of harmonics of ω are generated, but since we can assume $|\boldsymbol{M}_0| \gg |\boldsymbol{M}_1|, |\boldsymbol{H}_1|$, the problem is linearized. Since the original equation preserves the magnitude of $\boldsymbol{M}$ as a function of time, $|\boldsymbol{M}| = M_s$, we must have $|\boldsymbol{M}_0| = M_S$, and can represent the zeroth order magnetization by

$$\boldsymbol{M}_0 = M_S \boldsymbol{m}_0, \quad |\boldsymbol{m}_0| = 1 \quad (3.2)$$

The result of this decomposition is that the dynamics split in two equations (one for each order of magnitude, where we drop the time dependence $\mathrm{e}^{-\mathrm{i}\omega t}$ from the time harmonic fields)

$$\boldsymbol{0} = -\gamma \mu_0 M_S \boldsymbol{m}_0 \times \boldsymbol{H}_{\mathrm{eff},0} \quad (3.3)$$

$$-\mathrm{i}\omega \boldsymbol{M}_1 = -\gamma \mu_0 M_S \left[\boldsymbol{M}_1 \times \boldsymbol{H}_{\mathrm{eff},0}/M_S + \boldsymbol{m}_0 \times \boldsymbol{H}_{\mathrm{eff},1} \right] - \mathrm{i}\omega\alpha \boldsymbol{m}_0 \times \boldsymbol{M}_1 \quad (3.4)$$

We now turn to the solution of these equations.

3.1 Zeroth order solution

For a given ferromagnetic particle occupying a closed region Ω, the first equation is part of *Brown's equations* in micromagnetics [7, p. 27]

$$\begin{cases} \boldsymbol{m}_0 \times \boldsymbol{H}_{\mathrm{eff},0} = \boldsymbol{0} & \text{in } \Omega \\ \hat{\boldsymbol{n}} \cdot \nabla \boldsymbol{m}_0 = \boldsymbol{0} & \text{on } \partial\Omega \\ |\boldsymbol{m}_0| = 1 \end{cases} \quad (3.5)$$

Shape	$\mathbf{N}$
Spherical	$\begin{pmatrix} 1/3 & 0 & 0 \\ 0 & 1/3 & 0 \\ 0 & 0 & 1/3 \end{pmatrix}$
Circular needle	$\begin{pmatrix} 1/2 & 0 & 0 \\ 0 & 1/2 & 0 \\ 0 & 0 & 0 \end{pmatrix}$
Plate	$\begin{pmatrix} 0 & 0 & 0 \\ 0 & 0 & 0 \\ 0 & 0 & 1 \end{pmatrix}$

Table 2: Different demagnetization tensors for different shapes.

where $\hat{\boldsymbol{n}}$ denotes the outward unit normal of Ω. The boundary condition is due to the occurrence of the exchange term in the effective magnetic field, $\boldsymbol{H}_{\mathrm{ex}} = \lambda_{\mathrm{ex}} \nabla^2 \boldsymbol{M}$. The classical magnetic field $\boldsymbol{H}_0$ must satisfy Maxwell's static equations for a magnetized body [7, p. 22]

$$\begin{cases} \nabla \cdot \boldsymbol{H}_0 = -M_{\mathrm{S}} \nabla \cdot \boldsymbol{m}_0 & \text{in } \Omega \\ \nabla \cdot \boldsymbol{H}_0 = 0 & \text{outside } \Omega \\ \nabla \times \boldsymbol{H}_0 = \boldsymbol{0} & \text{everywhere} \end{cases} \tag{3.6}$$

with the boundary conditions on $\partial \Omega$

$$\begin{cases} \hat{\boldsymbol{n}} \cdot [\boldsymbol{H}_0] = M_{\mathrm{S}} \hat{\boldsymbol{n}} \cdot \boldsymbol{m}_0 \\ \hat{\boldsymbol{n}} \times [\boldsymbol{H}_0] = \boldsymbol{0} \end{cases} \tag{3.7}$$

where $[\boldsymbol{H}_0]$ denotes the jump of $\boldsymbol{H}_0$ across the boundary $\partial \Omega$. The equations (3.5) and (3.6) couple through $\boldsymbol{m}_0$ and the effective field

$$\boldsymbol{H}_{\mathrm{eff},0} = \boldsymbol{H}_0 - M_{\mathrm{S}} \mathbf{N}_{\mathrm{c}} \boldsymbol{m}_0 + \lambda_{\mathrm{ex}} M_{\mathrm{S}} \nabla^2 \boldsymbol{m}_0 \tag{3.8}$$

where we skip the magnetoelastic contribution $\boldsymbol{H}_{\mathrm{me},0}$. The combined equations are nonlinear and difficult to solve even numerically; this is the field of computational micromagnetics [8]. In general, the resulting magnetization direction $\boldsymbol{m}_0$ will vary within the magnetic particle.

Significant simplifications are possible for the special case of a spheroidal particle immersed in a homogeneous external field $\boldsymbol{H}_0^{\mathrm{e}}$. For this particular geometry, the particle is uniformly magnetized, and the total classical field within the particle can be shown to be

$$\boldsymbol{H}_0 = \boldsymbol{H}_0^{\mathrm{e}} - M_{\mathrm{S}} \mathbf{N}_{\mathrm{d}} \boldsymbol{m}_0 \tag{3.9}$$

where $\mathbf{N}_{\mathrm{d}}$ is the demagnetization tensor for the particle. A table of demagnetization tensors for different extremes of spheroidal particles is found in Table 2.

Since the particle is uniformly magnetized, the exchange term drops out, and the effective field is

$$\boldsymbol{H}_{\text{eff},0} = \boldsymbol{H}_0^{\text{e}} - M_{\text{S}}(\mathbf{N}_{\text{d}} + \mathbf{N}_{\text{c}})\boldsymbol{m}_0 = \boldsymbol{H}_0^{\text{e}} - M_{\text{S}}\mathbf{N}\boldsymbol{m}_0 \tag{3.10}$$

Brown's equations (3.5) require that the effective field is parallel to $\boldsymbol{m}_0$, that is, $\boldsymbol{H}_{\text{eff},0} = \beta M_{\text{S}}\boldsymbol{m}_0$ for some constant β, which implies

$$\boldsymbol{H}_0^{\text{e}}/M_{\text{S}} - \mathbf{N}\boldsymbol{m}_0 = \beta\boldsymbol{m}_0 \quad \Rightarrow \quad \boldsymbol{m}_0 = (\beta\mathbf{I} + \mathbf{N})^{-1}\boldsymbol{H}_0^{\text{e}}/M_{\text{S}} \tag{3.11}$$

The constant β is then determined from the normalization requirement $|\boldsymbol{m}_0| = 1$. Thus, the "constant" β is really a function of $\boldsymbol{H}_0^{\text{e}}$, as well as M_{S} and $\mathbf{N}$. Typically, it is of unit order (or of order $|\boldsymbol{H}_0^{\text{e}}|/M_{\text{S}}$ for strong bias), and together with the direction of $\boldsymbol{m}_0$ it is the primary parameter that can be controlled by an external field.

In the special case of the spherical particle, where $\mathbf{N} = \mathbf{I}/3$, we can solve (3.11) explicitly for $\beta = \pm|\boldsymbol{H}_0^{\text{e}}|/M_{\text{S}} - 1/3$. In order to choose the correct sign in this solution, we study the total free energy, $i.e.$, the sum of the anisotropy energy U_{an} and the magnetostatic energy of the particle [20, p. 157]

$$\mathcal{F}_{\text{tot}} = \int \left(U_{\text{an}} - \frac{\mu_0}{2}\boldsymbol{M}_0 \cdot (\boldsymbol{H}_0 + \boldsymbol{H}_0^{\text{e}})\right) dV = \frac{\mu_0}{2}\int \boldsymbol{M}_0 \cdot (\mathbf{N}_{\text{c}}\boldsymbol{M}_0 - \boldsymbol{H}_0 - \boldsymbol{H}_0^{\text{e}}) \, dV$$

$$= -\frac{\mu_0}{2}\int \boldsymbol{M}_0 \cdot (\boldsymbol{H}_{\text{eff},0} + \boldsymbol{H}_0^{\text{e}}) \, dV \tag{3.12}$$

which should be minimal for the correct β. This discards the minus sign, and henceforth we use the solution $\beta = |\boldsymbol{H}_0^{\text{e}}|/M_{\text{S}} - 1/3$.

In a composite material as in Figure 1, the "bias" field $\boldsymbol{H}_0^{\text{e}}$ at one particle may also be generated by the neighboring particles. Indeed, assuming that all particles have the same magnetization $\boldsymbol{M}_0$, the effective magnetization in the composite medium is $\boldsymbol{M}_0' = f_1\boldsymbol{M}_0$, where f_1 is the volume fraction of the magnetic particles. The field from the neighboring particles can then be estimated by [12, p. 162]

$$\boldsymbol{H}_0^{\text{e}} = \boldsymbol{H}_0^{\text{e}'} + \frac{1}{3}\boldsymbol{M}_0' = \boldsymbol{H}_0^{\text{e}'} + \frac{f_1}{3}\boldsymbol{M}_0 \tag{3.13}$$

where $\boldsymbol{H}_0^{\text{e}'}$ is the external field applied to the composite material. Inserting this in the expression for β, we find

$$\beta = \frac{|\boldsymbol{H}_0^{\text{e}}|}{M_{\text{S}}} - \frac{1}{3} = \frac{|\boldsymbol{H}_0^{\text{e}'}|}{M_{\text{S}}} - \frac{1 - f_1}{3} = \frac{|\boldsymbol{H}_0^{\text{e}'}|}{M_{\text{S}}} - \frac{f_2}{3} \tag{3.14}$$

where $f_2 = 1 - f_1$ is the volume fraction of the medium inbetween the particles. This demonstrates that as the volume fraction of the background material $f_2 \to 0$, $i.e.$, the composite material consists only of magnetic material, the bias parameter β is proportional to the field $\boldsymbol{H}_0^{\text{e}'}$. This field may in its turn consist of a demagnetizing field from discontinuities of the composite medium, but we study only an infinite medium here.

3.2   First order solution

We remind ourselves that the equation for the first order quantity $\boldsymbol{M}_1$ is

$$-\mathrm{i}\omega\boldsymbol{M}_1 = -\gamma\mu_0 M_\mathrm{S}[\boldsymbol{M}_1 \times \boldsymbol{H}_{\mathrm{eff},0}/M_\mathrm{S} + \boldsymbol{m}_0 \times \boldsymbol{H}_{\mathrm{eff},1}] - \mathrm{i}\omega\alpha\boldsymbol{m}_0 \times \boldsymbol{M}_1 \qquad (3.15)$$

Introducing $\omega_\mathrm{S} = \gamma\mu_0 M_\mathrm{S}$ and using $\boldsymbol{H}_{\mathrm{eff},0}/M_\mathrm{S} = \beta\boldsymbol{m}_0$, this can be written

$$\mathrm{i}\omega\boldsymbol{M}_1 = \omega_\mathrm{S}[\boldsymbol{M}_1 \times \beta\boldsymbol{m}_0 + \boldsymbol{m}_0 \times \boldsymbol{H}_{\mathrm{eff},1}] + \mathrm{i}\omega\alpha\boldsymbol{m}_0 \times \boldsymbol{M}_1 \qquad (3.16)$$

The effective field is

$$\boldsymbol{H}_{\mathrm{eff},1} = \boldsymbol{H}_1 - \mathbf{N}_\mathrm{c}\boldsymbol{M}_1 + \lambda_{\mathrm{ex}}\nabla^2\boldsymbol{M}_1 \qquad (3.17)$$

where $\boldsymbol{H}_1$ is the classical magnetic field appearing in Maxwell's equations. In the following, we ignore the exchange field, but return to its effects in Section 5. The small signal susceptibility is the relation between the small signal field $\boldsymbol{H}_1$ and the small signal magnetization $\boldsymbol{M}_1$. To find this, we rewrite (3.15) as

$$[\mathrm{i}\omega + \boldsymbol{m}_0 \times ((\omega_\mathrm{S}\beta - \mathrm{i}\alpha\omega)\mathbf{I} + \omega_\mathrm{S}\mathbf{N}_\mathrm{c})]\,\boldsymbol{M}_1 = \omega_\mathrm{S}\boldsymbol{m}_0 \times \boldsymbol{H}_1 \qquad (3.18)$$

From the structure of this equation it is seen that $\boldsymbol{m}_0 \cdot \boldsymbol{M}_1 = 0$, which means we only need to consider components orthogonal to $\boldsymbol{m}_0$. The equation is then a 2×2 system of linear equations, which can be solved explicitly after some algebra. The result is that the small signal susceptibility, defined by $\boldsymbol{M}_1 = \boldsymbol{\chi}\boldsymbol{H}_1$, is

$$\begin{pmatrix} \chi_{11} & \chi_{12} \\ \chi_{21} & \chi_{22} \end{pmatrix} = \frac{1}{D}\begin{pmatrix} \beta + N_{\mathrm{c},22} - \mathrm{i}\alpha\omega/\omega_\mathrm{S} & -\mathrm{i}\omega/\omega_\mathrm{S} - N_{\mathrm{c},12} \\ \mathrm{i}\omega/\omega_\mathrm{S} - N_{\mathrm{c},12} & \beta + N_{\mathrm{c},11} - \mathrm{i}\alpha\omega/\omega_\mathrm{S} \end{pmatrix} \qquad (3.19)$$

where we used that the tensor $\mathbf{N}_\mathrm{c}$ is symmetric, *i.e.*, $N_{\mathrm{c},12} = N_{\mathrm{c},21}$, and the denominator is

$$D = -(\omega/\omega_\mathrm{S})^2 - N_{\mathrm{c},12}^2 + (\beta + N_{\mathrm{c},22} - \mathrm{i}\alpha\omega/\omega_\mathrm{S})(\beta + N_{\mathrm{c},11} - \mathrm{i}\alpha\omega/\omega_\mathrm{S}) \qquad (3.20)$$

When anisotropy can be ignored, the susceptibility simplifies to

$$\begin{pmatrix} \chi_{11} & \chi_{12} \\ \chi_{21} & \chi_{22} \end{pmatrix} = \frac{1}{-(\omega/\omega_\mathrm{S})^2 + (\beta - \mathrm{i}\alpha\omega/\omega_\mathrm{S})^2}\begin{pmatrix} \beta - \mathrm{i}\alpha\omega/\omega_\mathrm{S} & -\mathrm{i}\omega/\omega_\mathrm{S} \\ \mathrm{i}\omega/\omega_\mathrm{S} & \beta - \mathrm{i}\alpha\omega/\omega_\mathrm{S} \end{pmatrix} \qquad (3.21)$$

From this form (temporarily ignoring losses, *i.e.*, $\alpha = 0$) we would conclude that the resonance frequency of the susceptibility is given by the expression $\omega_{\mathrm{res}}/\omega_\mathrm{S} = \pm\sqrt{(\beta + N_{\mathrm{c},22})(\beta + N_{\mathrm{c},22}) - N_{\mathrm{c},12}^2}$. However, the resonance frequency should be related to the appropriate input signal (the signal to which the material responds to). For the case of a single spherical particle the relevant input signal is the external applied field $\boldsymbol{H}_1^\mathrm{e}$, which is the field we control. We should then look at the polarizability $\boldsymbol{\gamma}_\mathrm{m}$, which is the relation between the total magnetic dipole moment, $V\boldsymbol{M}_1$ where V is the volume of the particle, and the external field $\boldsymbol{H}_1^\mathrm{e}$, *i.e.*, $V\boldsymbol{M}_1 = \boldsymbol{\gamma}_\mathrm{m}\boldsymbol{H}_1^\mathrm{e}$. Since for small spheroidal particles $\boldsymbol{H}_1 = \boldsymbol{H}_1^\mathrm{e} - \mathbf{N}_\mathrm{d}\boldsymbol{M}_1$, a short calculation shows that the tensor $\boldsymbol{\gamma}_\mathrm{m}$ is given by (3.19) after adding the components of $\mathbf{N}_\mathrm{d}$ to the

components of $\mathbf{N}_c$, *i.e.*, substitute $\mathbf{N}_c \rightarrow \mathbf{N}_c + \mathbf{N}_d$. Assuming no anisotropy and a spherical particle, this is $\mathbf{N}_c + \mathbf{N}_d = \mathbf{I}/3$, and the resonance frequency of $\boldsymbol{\gamma}_m$ is then

$$\frac{\omega_{\mathrm{res}}}{\omega_{\mathrm{S}}} = \beta + \frac{1}{3} = \frac{|\boldsymbol{H}_0^{\mathrm{e}}|}{M_{\mathrm{S}}} \qquad (3.22)$$

This shows that the resonance frequency of a spherical particle can be controlled by an external bias field $\boldsymbol{H}_0^{\mathrm{e}}$. The general condition for the resonance frequency of an arbitrary spheroidal particle is known as Kittel's equation [15], and is obtained by setting the right hand side of (3.20) equal to zero after making the substitution $\mathbf{N}_c \rightarrow \mathbf{N}_c + \mathbf{N}_d$. It should be remembered that in composite media, the external field $\boldsymbol{H}_0^{\mathrm{e}}$ may have a large contribution from the neighboring magnetic particles according to the discussion leading to (3.14).

3.3 Magnetic losses

The losses are connected to the anti-hermitian part of the susceptibility tensor. After some algebra, this is found to be

$$\frac{\boldsymbol{\chi} - \boldsymbol{\chi}^\dagger}{2} = \frac{\mathrm{i}\alpha\omega/\omega_{\mathrm{S}}}{D'}$$
$$\cdot \begin{pmatrix} (1+\alpha^2)(\omega/\omega_{\mathrm{S}})^2 + N_{c,12}^2 + (\beta + N_{c,22})^2 & -(\mathrm{i}\omega + N_{c,12})(2\beta + N_{c,11} + N_{c,22}) \\ (\mathrm{i}\omega - N_{c,12})(2\beta + N_{c,11} + N_{c,22}) & (1+\alpha^2)(\omega/\omega_{\mathrm{S}})^2 + N_{c,12}^2 + (\beta + N_{c,11})^2 \end{pmatrix}$$
$$(3.23)$$

where

$$D' = \left[(\beta + N_{c,11})(\beta + N_{c,22}) - (1+\alpha^2)(\omega/\omega_{\mathrm{S}})^2 - N_{c,12}^2 \right]^2$$
$$+ \left[(2\beta + N_{c,11} + N_{c,22})\alpha\omega/\omega_{\mathrm{S}} \right]^2 \quad (3.24)$$

A natural quantity for discussing losses is the magnetic conductivity, which is defined in [3] as $\boldsymbol{\sigma}_m = -\mathrm{i}\omega\mu_0(\boldsymbol{\chi} - \boldsymbol{\chi}^\dagger)/2$. Although this has unit $[\boldsymbol{\sigma}_m] = \Omega/m$ instead of S/m as in the electric case, we keep the notation from [3]. For simplicity we only give the special case $\mathbf{N}_c = \mathbf{0}$ here,

$$\boldsymbol{\sigma}_m = -\mathrm{i}\omega\mu_0\frac{\boldsymbol{\chi} - \boldsymbol{\chi}^\dagger}{2} = \frac{\alpha\mu_0\omega_{\mathrm{S}}(\omega/\omega_{\mathrm{S}})^2}{(\beta^2 - (1+\alpha^2)(\omega/\omega_{\mathrm{S}})^2)^2 + 4\alpha^2(\omega/\omega_{\mathrm{S}})^2\beta^2}$$
$$\cdot \begin{pmatrix} (1+\alpha^2)(\omega/\omega_{\mathrm{S}})^2 + \beta^2 & -2\mathrm{i}\beta\omega/\omega_{\mathrm{S}} \\ 2\mathrm{i}\beta\omega/\omega_{\mathrm{S}} & (1+\alpha^2)(\omega/\omega_{\mathrm{S}})^2 + \beta^2 \end{pmatrix} \quad (3.25)$$

It is seen that for the special case of $\beta = 0$, this is independent of frequency:

$$\boldsymbol{\sigma}_m \overset{\beta=0}{=} \mu_0\omega_{\mathrm{S}}\frac{\alpha}{1+\alpha^2}\mathbf{I} \qquad (3.26)$$

From Table 1 we see that typical intrinsic precession frequencies f_{S} are in the order 10–60 GHz, and we can expect $\alpha \approx 0.1$. Using $f_{\mathrm{S}} = 30$ GHz, the typical size of the magnetic conductivity is then

$$\sigma_m = \mu_0\omega_{\mathrm{S}}\frac{\alpha}{1+\alpha^2} \approx 4\pi \cdot 10^{-7} \cdot 2\pi \cdot 30 \cdot 10^9 \cdot 0.1\,\Omega/m = 2.4 \cdot 10^4\,\Omega/m \qquad (3.27)$$

In [27], it is shown that a sheet with magnetic material can be modeled with a series resistance of $\sigma_{\mathrm{m}}d$, where d is the thickness of the sheet, in a transmission line model of plane wave propagation. A perfect match to free space is then obtained if this resistance equals the wave impedance in vacuum, η_0, which requires the typical thickness $d = \eta_0/\sigma_{\mathrm{m}} = 377/(2.4 \cdot 10^4)\,\mathrm{m} = 1.6\,\mathrm{cm}$. This would be the typical thickness required for a sheet used as a magnetic absorber [25].

4   Eddy currents

So far, we have not discussed the possibility of the time varying external field to induce currents in the particle. Due to the linearity property for the small signal analysis, this can be considered in addition to the previous calculations. We first give the general equations in the quasi-static limit, and then the necessary approximations to get an estimate of the effects.

The quasi-static equations are the result from ignoring the displacement current $-\mathrm{i}\omega\boldsymbol{D}$ in Maxwell's equations,

$$\nabla \times \boldsymbol{E}_1 = \mathrm{i}\omega\boldsymbol{B}_1 = \mathrm{i}\omega\mu_0(\mathbf{I} + \boldsymbol{\chi})\boldsymbol{H}_1 \tag{4.1}$$

$$\nabla \times \boldsymbol{H}_1 = -\mathrm{i}\omega\boldsymbol{D}_1 + \boldsymbol{J}_1 \approx \sigma\boldsymbol{E}_1 \tag{4.2}$$

where we use the index 1 to indicate small signal quantities as in the previous section. Taking the curl of the last equation implies

$$\nabla \times (\nabla \times \boldsymbol{H}_1) = \mathrm{i}\omega\sigma\mu_0(\mathbf{I} + \boldsymbol{\chi})\boldsymbol{H}_1 \tag{4.3}$$

i.e., we have a diffusion equation for the magnetic field.

From this equation it is seen that the typical length scale is given by the skin depth, $\delta_{\mathrm{s}} = \sqrt{2/(\omega\sigma\mu_0)}$. Ferromagnetic materials like iron often have a high conductivity, on the order of $10^7\,\mathrm{S/m}$. The skin depth at $10\,\mathrm{GHz}$ is then

$$\delta_{\mathrm{s}} = \sqrt{\frac{2}{\omega\sigma\mu_0}} \approx 1.6\,\mu\mathrm{m} \tag{4.4}$$

This is not too far from the typical size of the particle, $100\,\mathrm{nm}$ or less. If the susceptibility $\boldsymbol{\chi}$ is not too large, the particle size is roughly one order of magnitude less than the skin depth. This does not automatically mean that the induced field is small, but at least motivates ignoring the skin effect when doing our calculations.

A short calculation in Appendix A shows that if the magnetic field is constant throughout a spherical particle of radius R, the induced magnetization due to eddy currents is

$$\boldsymbol{m} = \mathrm{i}\omega\sigma R^5\frac{2\pi}{15}\boldsymbol{B} \tag{4.5}$$

Normalizing with the volume of the sphere, $4\pi R^3/3$, we find the magnetization due to induction (this should really be spatially varying, but we are only interested in orders of magnitude)

$$\boldsymbol{M}_{\mathrm{ind}} = \frac{\boldsymbol{m}}{4\pi R^3/3} = \mathrm{i}\omega\sigma R^2\frac{1}{10}\boldsymbol{B} = \frac{\mathrm{i}\omega\sigma\mu_0 R^2}{10}(\mathbf{I} + \boldsymbol{\chi})\boldsymbol{H}_1 \tag{4.6}$$

This should be compared to the magnetization induced through the susceptibility, which is $\boldsymbol{\chi H}_1$. This once again demonstrates the crucial dependence on the skin depth relative the particle dimensions. In our case, we calculate

$$\frac{\omega \sigma \mu_0 R^2}{10} \approx 2\pi \cdot 10^{10} \cdot 10^7 \cdot 4\pi \cdot 10^{-7}(0.1 \cdot 10^{-6})^2 \frac{1}{10} = 7.9 \cdot 10^{-4} \qquad (4.7)$$

which is indeed a small number. This demonstrates that the eddy currents can be controlled by the size of the particles. The effects of eddy currents are thus negligible compared to the effects derived from the Landau-Lifshitz-Gilbert equation for sufficiently small particles.

5   Spin waves

Before turning to the homogenization of ferromagnetic particles, we discuss the possibilities of spin waves. One usually distinguishes between two types of spin waves, *i.e.*, magnetostatic (Walker modes) and exchange modes. The former are observed in samples of large dimension where the exchange energy is negligible compared to the demagnetization energy. On the other hand, the exchange modes are obtained when at least one dimension of the sample is small, which means that the exchange energy will dominate and the demagnetization energy can be neglected.

In order to understand what type of spin modes that will be present it is important to explain the concept of small and large in this context. For particles small enough, it becomes energetically favorable to form a single domain particle, which means that exchange energy is dominating. However, as the dimensions of the particle increase, multidomains will form and the demagnetization energy will prevail. From nucleation-field calculations a critical radius of the sphere is obtained [6]. At this critical radius, the behaviour of the magnetization shift from the so called magnetization curling to rotation in unison, *i.e.*, from a multidomain particle to a singledomain particle. This critical radius is here found to be of the order $10\,\mathrm{nm}$. From measurements, this radius seems to be in the order of 10–$100\,\mathrm{nm}$ [21, 29]. Thus, the size range in which exchange modes are expected is typically for radius $R \leq 100\,\mathrm{nm}$, which is also mentioned in [2]. This limit is not distinct and there is an intermediate region where both modes exist (mode mixing), which is investigated in [1, 30]. In this section we study the so called exchange modes, *i.e.*, where the particle size is of the order $R \leq 100\,\mathrm{nm}$, and their influences on the permeability.

Spin waves are propagating disturbances of the collective precession of the magnetic spins in the ferromagnetic material. Thus, in an infinite medium we expect solutions of the form $\boldsymbol{M}_1 \mathrm{e}^{\mathrm{i}(\boldsymbol{k}\cdot\boldsymbol{x}-\omega t)}$ which can exist independent of a signal field $\boldsymbol{H}_1$. In [16, p. 506] the following dispersion relation is presented

$$\omega/\omega_{\mathrm{S}} = \beta + \lambda_{\mathrm{ex}}k^2 \qquad (5.1)$$

We see that if ω is in the order of ω_{S} and β is in the order of unity, k^2 is in the order of $1/\lambda_{\mathrm{ex}}$. This implies a typical wavelength of the spin waves of

$$\lambda \approx 2\pi\sqrt{\lambda_{\mathrm{ex}}} = 2\pi l_{\mathrm{ex}} \qquad (5.2)$$

where l_{ex} is the exchange length tabulated in Table 1. From this table, it is seen that the exchange length is in the order of 3–10 nm, which means the typical wavelength of the spin wave is around 20–60 nm. Since the typical single domain particle is smaller than 100 nm, this means resonant conditions for the spin wave can be established in the GHz range.

Note that the spin wave solution is formally independent of the solution induced by the signal field, and as such represent a solution of the homogeneous differential equation. Thus, if the signal field has a frequency corresponding to a resonant spin wave, we can expect strong coupling from the signal to the spin waves, which are ultimately dissipated in losses. This may be an interesting possibility of increasing the magnetic losses.

5.1 Excitation of exchange modes

In this section we study the excitation of exchange modes in a spherical particle due to a uniform external time harmonic magnetic field. Using (3.17) (with $\mathbf{N}_{\mathrm{c}} = 0$) in (3.16) we obtain

$$\left[\mathrm{i}\omega \mathbf{I} + \boldsymbol{m}_0 \times ((\omega_{\mathrm{S}}\beta - \mathrm{i}\alpha\omega - \lambda_{\mathrm{ex}}\omega_{\mathrm{S}}\nabla^2)\mathbf{I}) \right] \boldsymbol{M}_1 = \omega_{\mathrm{S}}\boldsymbol{m}_0 \times \boldsymbol{H}_1 \quad \text{in } \Omega \qquad (5.3)$$

where $\boldsymbol{H}_1 = \boldsymbol{H}_1^{\mathrm{e}} + \boldsymbol{H}_{M_1}$ is the sum of the external uniform applied field $\boldsymbol{H}_1^{\mathrm{e}}$ and the demagnetization field $\boldsymbol{H}_{M_1}$ due to the small signal magnetization. This is essentially the same equation as in [6, p. 59], only here we have neglected the crystalline volume anisotropy. In order to take the geometry of the particle into account, (5.3) needs to be supplemented with the appropriate boundary condition. The form of this boundary condition depends on whether the surface anisotropy is included or not. There are several ways to express this anisotropy.[1] According to [6, p. 59] the general boundary condition (to first order) is a Robin-like boundary condition. In [2] a uniaxial surface anisotropy energy density is suggested that leads to the following boundary condition

$$\hat{\boldsymbol{n}} \cdot \nabla \boldsymbol{M}_1 + \xi \boldsymbol{M}_1 = \boldsymbol{0} \quad \text{on } \partial\Omega \qquad (5.4)$$

where $\xi = \frac{2K_{\mathrm{s}}}{\lambda_{\mathrm{ex}}\mu_0 M_{\mathrm{s}}^2}$ is a pinning parameter and K_{s} is a surface anisotropy constant.

We choose the direction of the static magnetization $\boldsymbol{m}_0$ as the $\hat{\boldsymbol{z}}$-direction, *i.e.*, the small signal magnetization $\boldsymbol{M}_1$ will be small perturbations in the xy-plane. Now, assume that the small signal magnetization can be expressed as

$$\boldsymbol{M}_1 = \sum_{nlm}(a_{nlm}\boldsymbol{M}_{1,nlm}^+ + b_{nlm}\boldsymbol{M}_{1,nlm}^-) = \sum_{nlm}(a_{nlm}\frac{\hat{\boldsymbol{x}} + \mathrm{i}\hat{\boldsymbol{y}}}{\sqrt{2}} + b_{nlm}\frac{\hat{\boldsymbol{x}} - \mathrm{i}\hat{\boldsymbol{y}}}{\sqrt{2}})M_{1,nlm} \quad (5.5)$$

where the functions $M_{1,nlm}$ are eigenfunctions of the Laplace operator with the boundary condition (5.4),

$$\nabla^2 M_{1,nlm} = -k_{ln}^2 M_{1,nlm} \qquad (5.6)$$

$$\Rightarrow M_{1,nlm} = \mathrm{j}_l(k_{ln}r)\mathrm{Y}_{lm}(\theta, \phi) \qquad (5.7)$$

---

[1]It seems that it is not fully understood what type of surface anisotropy expression that actually occurs in real physical systems.

ξR	0.25	0.5	1	f_r(GHz)
x_{00}	0.8447	1.1656	1.5708	8.2
x_{01}	4.5490	4.6042	4.7124	3.5
x_{02}	7.7576	7.7899	7.8540	5.8
x_{11}	2.2862	2.4605	2.7437	7.0
x_{21}	3.4951	3.6328	3.8702	5.2
x_{31}	4.6433	4.7622	4.9734	2.9

Table 3: The eigenvalues x_{ln}, obtained from (5.11) and the associated resonance frequencies for a $R = 50\,\mathrm{nm}$ Co particle with $\xi R = 1$.

which is a complete system of expansion functions for the problem. Here $\mathrm{j}_l(k_{ln}r)$ denote the spherical Bessel functions and $\mathrm{Y}_{lm}(\theta, \phi)$ are the spherical harmonics. Inserting (5.5) into (5.3) and using the orthogonality of the $M_{1,nlm}$ functions, the following expressions for the mode coefficients is obtained

$$a_{nlm} = \frac{(\boldsymbol{H}_1, \boldsymbol{M}_{1,nlm}^+)}{(\boldsymbol{M}_{1,nlm}^+, \boldsymbol{M}_{1,nlm}^+)\left[\lambda_{\mathrm{ex}}k_{ln}^2 + \beta - \mathrm{i}\alpha\omega/\omega_{\mathrm{S}} - \omega/\omega_{\mathrm{S}}\right]} \tag{5.8}$$

$$b_{nlm} = \frac{(\boldsymbol{H}_1, \boldsymbol{M}_{1,nlm}^-)}{(\boldsymbol{M}_{1,nlm}^-, \boldsymbol{M}_{1,nlm}^-)\left[\lambda_{\mathrm{ex}}k_{ln}^2 + \beta - \mathrm{i}\alpha\omega/\omega_{\mathrm{S}} + \omega/\omega_{\mathrm{S}}\right]} \tag{5.9}$$

where the notation $(\boldsymbol{A}, \boldsymbol{B})$ denotes the inner product over the sphere.

With the boundary condition (5.4), the inner product becomes

$$(\boldsymbol{M}_{1,nlm}^\pm, \boldsymbol{M}_{1,nlm}^\pm) = \int_0^R \mathrm{j}_l^2(k_{ln}r)r^2\,\mathrm{d}r \int_0^{2\pi}\int_0^\pi \mathrm{Y}_{lm}(\theta, \phi)\mathrm{Y}_{lm}(\theta, \phi)^* \sin\theta\,\mathrm{d}\theta\,\mathrm{d}\phi$$

$$= \frac{R^3}{2}\left[(1 - \frac{l(l+1)}{x_{ln}^2})\mathrm{j}_l^2(x_{ln}) + \frac{\mathrm{j}_l(x_{ln})\mathrm{j}_l^{'}(x_{ln})}{x_{ln}} + \mathrm{j}_l^{'2}(x_{ln})\right] = \frac{R^3}{2}N_{ln} \quad (5.10)$$

where $x_{ln} = k_{ln}R$ are the roots of

$$x_{ln}\frac{\mathrm{dj}_l(x_{ln})}{\mathrm{d}x_{ln}} + R\xi\mathrm{j}_l(x_{ln}) = 0 \tag{5.11}$$

Some values of these roots are tabulated in Table 3, along with the associated resonance frequencies.

The inner product $(\boldsymbol{H}_1, \boldsymbol{M}_{1,nlm}^\pm)$ is given by

$$(\boldsymbol{H}_1, \boldsymbol{M}_{1,nlm}^\pm) = \boldsymbol{H}_1 \cdot \boldsymbol{M}_1^\pm \int_0^R \mathrm{j}_l(k_{ln}r)r^2\,\mathrm{d}r \int_0^{2\pi}\int_0^\pi \mathrm{Y}_{lm}(\theta, \phi)^* \sin\theta\,\mathrm{d}\theta\,\mathrm{d}\phi$$

$$= \begin{cases} 0 & l, m \neq 0 \\ \boldsymbol{H}_1 \cdot \boldsymbol{M}_1^\pm\sqrt{4\pi}\frac{R^3}{x_{0n}}\mathrm{j}_1(x_{0n}) & l, m = 0 \end{cases} \tag{5.12}$$

where $\boldsymbol{M}_1^\pm = \frac{\hat{\boldsymbol{x}} \pm i\hat{\boldsymbol{y}}}{\sqrt{2}}$. We now conclude that all mode coefficients are zero for indices $l, m \neq 0$, and the remaining ones are

$$a_{n00} = \frac{2\boldsymbol{H}_1 \cdot \boldsymbol{M}_1^+ \sqrt{4\pi} j_1(x_{0n})}{x_{0n} N_{0n} \left[(l_{\mathrm{ex}}/R)^2 x_{0n}^2 + \beta - i\alpha\omega/\omega_{\mathrm{S}} - \omega/\omega_{\mathrm{S}}\right]} \tag{5.13}$$

$$b_{n00} = \frac{2\boldsymbol{H}_1 \cdot \boldsymbol{M}_1^- \sqrt{4\pi} j_1(x_{0n})}{x_{0n} N_{0n} \left[(l_{\mathrm{ex}}/R)^2 x_{0n}^2 + \beta - i\alpha\omega/\omega_{\mathrm{S}} + \omega/\omega_{\mathrm{S}}\right]} \tag{5.14}$$

where N_{0n} is given in (5.10).

Now we see the effect of the surface anisotropy on the mode coefficients a_{nml}, b_{nml} and hence, the magnetization (5.5). As ξ becomes very small, (5.11) becomes a Neumann condition, $i.e.$, $\frac{\mathrm{d}j_l(x_{ln})}{\mathrm{d}x_{ln}} = 0$, which then modifies the eigenvalues x_{ln}. The mode coefficients now all equal zero since $j_1(x_{0n}) = -j_0'(x_{0n}) = 0$, except for the case $x_{00} = 0$, where we obtain the uniform mode treated in Section 3.2. Thus, if there is no surface anisotropy and the applied small signal field is uniform, then only the uniform mode is present. The resonance frequency for this mode is independent of the radius of the particle (which is a typical property of the magnetostatic modes). For the case where we have surface anisotropy included it is seen that the exchange modes are excited. The magnetization will no longer precess in unison and the resonance frequency depends on the radius of the sphere. Thus, in order for exchange modes to occur when a uniform field is applied, surface anisotropy is needed ($i.e.$, pinning of the magnetization at the surface). The same conclusion is also found in for instance [14].

5.2 Magnetic susceptibility and spin wave resonance

For the case of a uniform applied field, the solution (5.5) together with (5.13) and (5.14), can be written in the following way

$$\boldsymbol{M}_1 = \boldsymbol{\chi}\boldsymbol{H}_1 = \sum_n \boldsymbol{\chi}_n \boldsymbol{H}_1 \tag{5.15}$$

where $\boldsymbol{\chi}$ is the total susceptibility tensor which consists of a sum of mode susceptibility tensors, one for each mode. If this tensor is represented in an $\hat{\boldsymbol{x}}$-$\hat{\boldsymbol{y}}$ base then we have

$$\boldsymbol{\chi}_n = \frac{M_{0n} j_0(k_{0n}r)}{((l_{\mathrm{ex}}/R)^2 x_{0n}^2 + \beta - i\alpha\omega/\omega_{\mathrm{S}})^2 - (\omega/\omega_{\mathrm{S}})^2}$$
$$\cdot \begin{pmatrix} (l_{\mathrm{ex}}/R)^2 x_{0n}^2 + \beta - i\alpha\omega/\omega_{\mathrm{S}} & -i\omega/\omega_{\mathrm{S}} \\ i\omega/\omega_{\mathrm{S}} & (l_{\mathrm{ex}}/R)^2 x_{0n}^2 + \beta - i\alpha\omega/\omega_{\mathrm{S}} \end{pmatrix} \tag{5.16}$$

where $M_{0n} = \frac{2j_1(x_{0n})}{x_{0n} N_{0n}}$. In particular, it is found that the resonance frequencies for the different modes (for small losses, $i.e.$, $\alpha^2 \ll 1$) are given by

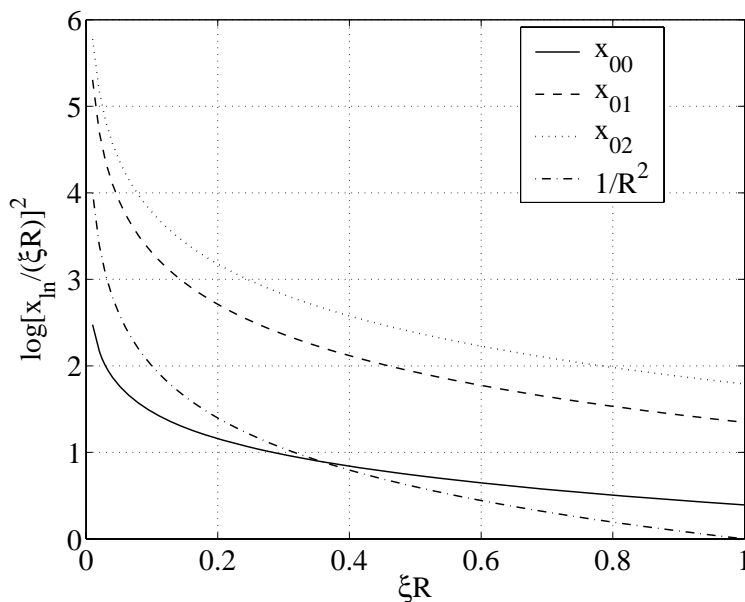$$\pm\omega/\omega_{\mathrm{S}} = (l_{\mathrm{ex}}/R)^2 x_{0n}^2 + \beta \tag{5.17}$$

Figure 2: The logarithm of x_{ln}^2/R^2 for a particle with radius R. The values for x_{ln} are computed from (5.11) and plotted against ξR, where $\xi = \frac{2K_s}{\lambda_{ex}\mu_0 M_s^2}$.

which agrees with the expression in [2] except here we omitted the crystalline anisotropy. If the easy axis of the crystalline anisotropy coincides with the direction of the magnetization $\boldsymbol{M}_0$, it can easily be included by adding N_c and the result is simply a shift in the resonance frequencies.

To be consistent with the choice of input signal in section 3.2 we should apply the polarizability rather than the susceptibility when studying the resonance frequency. But since the boundary condition (5.4) leads to a nonuniform magnetization $\boldsymbol{M}_1$ we no longer have a uniform demagnetization field $\boldsymbol{H}_{M_1}$. Therefore, in order to obtain the polarizability, we cannot simply follow the procedure in section 3.2 leading to (3.22). Taking the effects of the nonuniform $\boldsymbol{H}_{M_1}$ into account leads to extensive calculations [1, 30]. However, the effects of the demagnetization field $\boldsymbol{H}_{M_1}$ in the nonuniform case will be weaker and can, as a first approximation, be neglected. Hence, we set $\boldsymbol{H}_1 \approx \boldsymbol{H}_1^e$ and discuss only the resonances of the susceptibility $\boldsymbol{\chi}$ for simplicity.

From (5.17) one might expect that the resonance frequency has a $1/R^2$ dependence. However, this is in general not the case. The reason for this is that the x_{ln} themselves has a R dependence as can be seen from Figure 2. Here, we see that only for small values of ξR, a $1/R^2$ dependence can be expected. This deviation from $1/R^2$ dependence is also found in experiments [21, 29] and thus could be explained by the surface anisotropy, *i.e.*, pinning of the spins at the surface of the particle. In [29], the resonance frequency for Co is found to have a $R^{-0.66}$ dependence and according to [2] this behavior can be expected theoretically for $\xi R \approx 1$. For a given radius of the particle, it is then possible to estimate the surface anisotropy. Using a radius of 50 nm gives a surface anisotropy $K_s \approx 2 \cdot 10^{-4}$ J/m^2 which, according to [2],
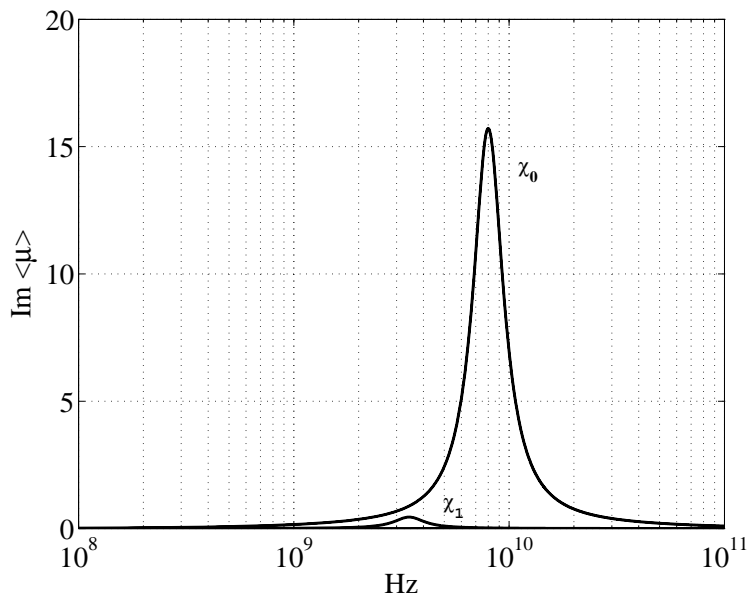
Figure 3: The imaginary part of the diagonal element of the mode permeability tensors averaged over a Co particle with $R = 50$ nm. The material parameters are taken from Table 1, $\alpha = 0.2$, $\xi R = 1$ and the bias field was set to $H_0^{\mathrm{e}} = M_{\mathrm{s}}/8$.

is of the same order as obtained from ferromagnetic resonance data for $\mathrm{Ni}_{0.84}\mathrm{Co}_{0.16}$ films.

In Figure 3 the material properties in Table 1 for Co have been used to plot the imaginary part of the diagonal element of the permeability. For a uniform small signal field $\boldsymbol{H}_1$ we have, according to (5.13) and (5.14), that only modes with index $l = 0$ will exist. From Figure 3 we see that only the mode with $n = l = 0$ gives a substantial contribution to the permeability. However, in reality, the shape of the particle will deviate from the ideal spherical geometry, resulting in perturbations in the uniform small signal field. Thus, in a composite material with ferromagnetic particles of some random irregular shape, the applied field at a particle will not be completely uniform. This means that we can expect modes with index $l \neq 0$ to be excited and from Table 3 we see that some of these modes are resonant in the GHz range. Indeed, comparing with the results from the measurements in [21, 29], we see that this behavior can be expected and that these higher order modes are important in terms of absorption.

6 Homogenization

In this paper we study the effective magnetic properties of a composite material consisting of ferromagnetic inclusions in a background material. By assuming that the direction of magnetization is exactly the same in each particle, we can use standard homogenization formulas, such as the Hashin-Shtrikman, also known as the Maxwell-Garnett formula [26]. This formula is exact in the situation depicted in
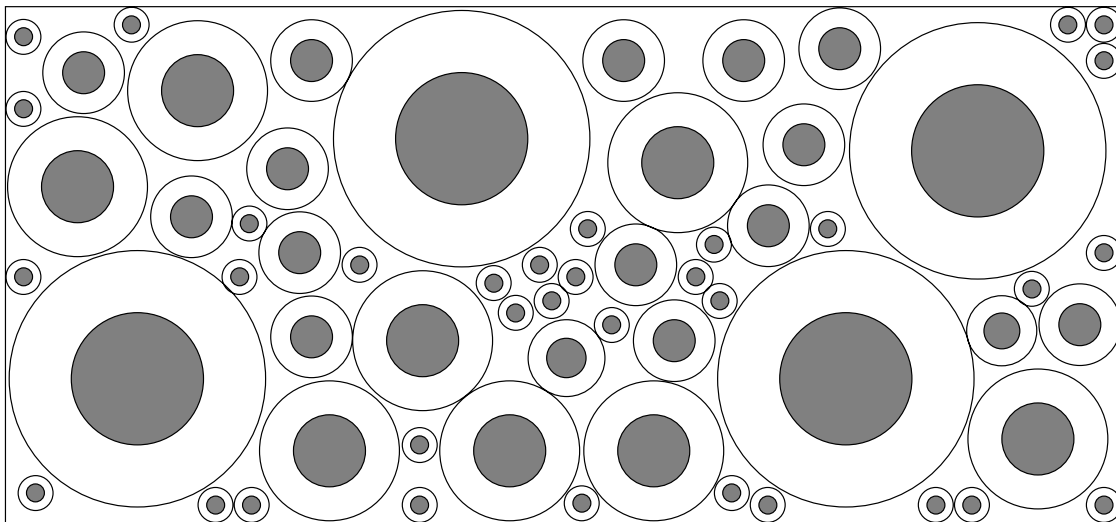
Figure 4: A geometry which gives the exact result for the Hashin-Shtrikman formula (6.1). The entire bulk medium is made up of coated spheres of varying sizes, but with the same volume ratio between the materials. Here, only a few sizes are represented and the medium is not completely filled. This is usually a good approximation for a geometry which really consists of spherical inclusions in a background material.

Figure 4, *i.e.*, coated ellipsoids, where each ellipsoid has the same volume ratio between the two different materials. This is often a good approximation to the microgeometry we study, where we have spherical inclusions in a background material. Assuming that the surrounding material has the isotropic permeability $\boldsymbol{\mu}_2 = \mu_2\mathbf{I}$ and the inclusions have the isotropic permeability $\boldsymbol{\mu}_1 = \mu_1\mathbf{I}$, the scalar version of this formula is

$$\mu_{\text{eff}} = \mu_2 + \frac{f_1\mu_2(\mu_1 - \mu_2)}{\mu_2 + (f_2/3)(\mu_1 - \mu_2)} \tag{6.1}$$

If we instead assume that the inclusions have the non-isotropic permeability $\boldsymbol{\mu}_1$, the tensor version of this formula is [23, p. 145]

$$\boldsymbol{\mu}_{\text{eff}} = \mu_2\mathbf{I} + f_1\mu_2(\boldsymbol{\mu}_1 - \mu_2\mathbf{I})[\mu_2\mathbf{I} + (f_2/3)(\boldsymbol{\mu}_1 - \mu_2\mathbf{I})]^{-1} \tag{6.2}$$

If the inclusions are not spherical, the tensor multiplying f_2 in this formula must be slightly changed, see [23] for details.

In Appendix B we show that the eigenvectors of the effective permeability defined by (6.2) are the same as the eigenvectors of the tensor $\boldsymbol{\mu}_1$, which means we can simply apply the scalar formula (6.1) to the eigenvalues in order to compute the effective material parameters.

6.1 Calculation of effective material parameters

In [18] it is shown that when mixing a Lorentz material with a non-dispersive material using formula (6.1), the resulting material also has a Lorentz resonance, but

the resonance frequency is shifted to a higher value. A more general result of [18] is that if the permittivity of material 1 can be written

$$\epsilon_1(\omega) = \frac{\sum_m a_m \omega^m}{\sum_n b_n \omega^n}, \quad b_0 = 1 \tag{6.3}$$

and the formula (6.1) is used, the corresponding coefficients for the effective permittivity are given by

$$a_m^{\text{eff}} = \epsilon_2 \frac{(1 + 2f_1)a_m + 2\epsilon_2(1 - f_1)b_m}{(1 - f_1)a_0 + \epsilon_2(2 + f_1)}, \qquad m = 0, 1, 2, \dots \tag{6.4}$$

$$b_0^{\text{eff}} = 1 \tag{6.5}$$

$$b_m^{\text{eff}} = \frac{(1 - f_1)a_n + \epsilon_2(2 + f_1)b_n}{(1 - f_1)a_0 + \epsilon_2(2 + f_1)}, \qquad n = 1, 2, 3, \dots \tag{6.6}$$

In Appendix B, this result is used to find the frequency dependence of the eigenvalues of the effective permeability tensor. The result is then combined with knowledge of the eigenvectors (being circularly polarized waves), to find the following expression for the effective permeability:

$$\boldsymbol{\mu}_{\text{eff}} = \begin{pmatrix} \mu_{\text{eff}} & -\mathrm{i}\mu_{g,\text{eff}} & 0 \\ \mathrm{i}\mu_{g,\text{eff}} & \mu_{\text{eff}} & 0 \\ 0 & 0 & \mu_{z,\text{eff}} \end{pmatrix} \tag{6.7}$$

where the entries are given by

$$\mu_{\text{eff}} = \frac{a_0^{\text{eff}} - \frac{\mathrm{i}\alpha\omega}{\beta\omega_b}\left(a_0^{\text{eff}} + \frac{\omega_b}{\omega_a}\right) - (1 + \alpha^2)\frac{\omega^2}{\beta^2\omega_a\omega_b}}{\left(1 - \frac{\mathrm{i}\alpha\omega}{\beta\omega_b}\right)^2 - \frac{\omega^2}{\beta^2\omega_b^2}} \tag{6.8}$$

$$\mu_{g,\text{eff}} = \frac{\left(a_0^{\text{eff}} - \frac{\omega_b}{\omega_a}\right)\frac{\omega}{\beta\omega_b}}{\left(1 - \frac{\mathrm{i}\alpha\omega}{\beta\omega_b}\right)^2 - \frac{\omega^2}{\beta^2\omega_b^2}} \tag{6.9}$$

$$\mu_{z,\text{eff}} = \mu_2 + \frac{3f_1\mu_2(1 - \mu_2)}{3\mu_2 + (1 - f_1)(1 - \mu_2)} \overset{\mu_2=1}{=} 1 \tag{6.10}$$

with

$$a_0^{\text{eff}} = \mu_2 \frac{(1 + 2f_1)(1 + 1/\beta) + 2\mu_2(1 - f_1)}{(1 - f_1)(1 + 1/\beta) + \mu_2(2 + f_1)} \overset{\mu_2=1}{=} 1 + \frac{f_1}{\beta + (1 - f_1)/3} \tag{6.11}$$

$$\omega_a = \frac{\omega_S}{\mu_2} \frac{(1 - f_1)(1 + 1/\beta) + \mu_2(2 + f_1)}{(1 + 2f_1) + 2\mu_2(1 - f_1)} \overset{\mu_2=1}{=} \omega_S\left(1 + \frac{1 - f_1}{3\beta}\right) \tag{6.12}$$

$$\omega_b = \omega_S \frac{(1 - f_1)(1 + 1/\beta) + \mu_2(2 + f_1)}{(1 - f_1) + \mu_2(2 + f_1)} \overset{\mu_2=1}{=} \omega_S\left(1 + \frac{1 - f_1}{3\beta}\right) \tag{6.13}$$

In the above formulas, we have given special attention to the case $\mu_2 = 1$, since this is a common case in practice and leads to substantial simplifications. We now proceed to give some interpretations of these formulas, restricting ourselves to the case $\mu_2 = 1$ for simplicity.

6.2 Resonance frequency and losses

As pointed out in section 3.2, when discussing the resonance frequency of the material it is important to associate it with the proper input signal. In the case of the single particle we concluded that the relevant input signal is the field external to the particle, $\boldsymbol{H}_1^{\mathrm{e}}$. In the infinite composite material, this corresponds to the field inside the composite, $\boldsymbol{H}_1$, making the effective permittivity $\boldsymbol{\mu}_{\mathrm{eff}}$ the relevant quantity to study if we want to compare the resonances for the two cases. Examining (6.8) and (6.9) it is identified that the resonance frequency for a composite material is given by (for $\alpha = 0$)

$$\omega_{\mathrm{res}} = \beta \omega_b = \omega_{\mathrm{S}}\left(\beta + \frac{1 - f_1}{3}\right) \tag{6.14}$$

and using $\beta = \frac{|\boldsymbol{H}_0^{\mathrm{e}\prime}|}{M_{\mathrm{S}}} - \frac{f_2}{3}$ from (3.14) we obtain

$$\beta \omega_b = \omega_{\mathrm{S}}\frac{|\boldsymbol{H}_0^{\mathrm{e}\prime}|}{M_{\mathrm{S}}} = \gamma \mu_0 |\boldsymbol{H}_0^{\mathrm{e}\prime}| \tag{6.15}$$

We see that the resonance frequency for the composite is independent of the volume fraction f_1. From the expression in (3.22) we see that the resonance frequency for a single spherical particle is given by $\omega_{\mathrm{S}}(\beta + 1/3)$, where $\beta = \frac{|\boldsymbol{H}_0^{\mathrm{e}\prime}|}{M_{\mathrm{S}}} - 1/3$ for the single particle ($f_2 = 0$). We conclude that, when subjected to the same external bias field, the resonance frequency for the composite is equal to that of a single spherical particle and independent of the volume fraction f_1, a result which has been verified experimentally [29].

This result is in contrast with what is known for the frequency dependence of dielectric composite materials. As is seen in [18], the resonance frequency of a composite material with Lorentz material inclusions, is usually higher than the resonance frequency of the inclusions. In our case, the resonance frequency is determined primarily by the strength of the static magnetic bias field, which may depend implicitly on the volume fraction due to possible demagnetization contributions from discontinuities in the composite material.

Turning our attention to the magnetic losses, the effective magnetic conductivity is found to be (after some algebra)

$$\boldsymbol{\sigma}_{\mathrm{m,eff}} = -\mathrm{i}\omega\mu_0 \frac{\boldsymbol{\mu}_{\mathrm{eff}} - \boldsymbol{\mu}_{\mathrm{eff}}^\dagger}{2} = \frac{\alpha\mu_0\beta\omega_b\omega^2(a_0^{\mathrm{eff}} - 1)}{((\beta\omega_b)^2 - (1 + \alpha^2)\omega^2)^2 + 4\alpha^2\omega^2(\beta\omega_b)^2}$$
$$\cdot \begin{pmatrix} (1 + \alpha^2)\omega^2 + (\beta\omega_b)^2 & -2\mathrm{i}\beta\omega_b\omega \\ 2\mathrm{i}\beta\omega_b\omega & (1 + \alpha^2)\omega^2 + (\beta\omega_b)^2 \end{pmatrix} \tag{6.16}$$

This result is only given for the x and y components since all z parts are zero. The only change necessary to include the case $\mu_2 \neq 1$ is $a_0^{\mathrm{eff}} - 1 \rightarrow a_0^{\mathrm{eff}} - \omega_b/\omega_a$. It is seen that for the special bias condition $\beta\omega_b = 0$, the effective magnetic conductivity is independent of frequency and becomes

$$\boldsymbol{\sigma}_{\mathrm{m,eff}} = \mu_0\omega_{\mathrm{S}}f_1\frac{\alpha}{1 + \alpha^2}\mathbf{I}, \quad \text{when} \quad \beta\omega_b = 0, \, \mu_2 = 1 \tag{6.17}$$
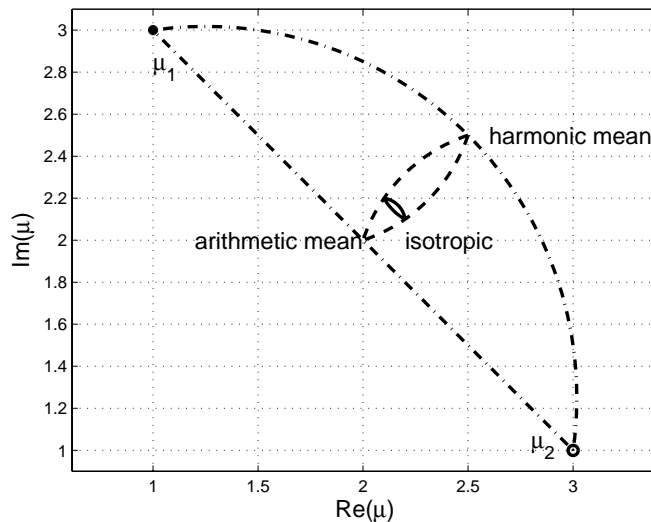
Figure 5: Example of bounds in the complex plane for a diagonal element of the effective permeability. With no information on the volume fraction, the effective permeability μ_{eff} must be inside the dash-dotted curves. If the volume fraction is known, μ_{eff} must be inside the dashed curves, and if we also know the effective medium is isotropic, μ_{eff} must be inside the solid curves.

The condition $\beta\omega_b = 0$ corresponds to the external magnetic bias field $\boldsymbol{H}_0^{\text{e}\prime}$ being zero according to (6.15). For the case $f_1 = 1$, *i.e.*, the magnetic material fills up the entire composite, it is readily seen that we get the magnetic conductivity given by (3.26), as expected. Also note that the magnetic conductivity depends on the damping constant α and is proportional to the saturation magnetization M_{S} via ω_{S}.

6.3   Bounds in the complex plane

When calculating the effective properties of composite materials consisting of two (or more) component materials, it is well understood that formulas like (6.1) and (6.2) are only approximations, which can be more or less accurate depending on the precise microstructure of the composite material. However, one thing that is not so well understood is that they can be used to form bounds for the effective material parameters, not only for real valued parameters but also in the complex plane [9, 22, 23]. The theory may appear intricate, but the recipe is simple and is given a very short presentation here.

Due to the analytical properties of the effective material parameters as functions of the component parameters, it is for each fixed frequency possible to define a region in the complex plane wherein a diagonal element of the effective permeability must take its value. By a diagonal element μ, we mean the quadratic form

$$\mu = \frac{\boldsymbol{H}^* \cdot (\boldsymbol{\mu}\boldsymbol{H})}{|\boldsymbol{H}|^2} \tag{6.18}$$
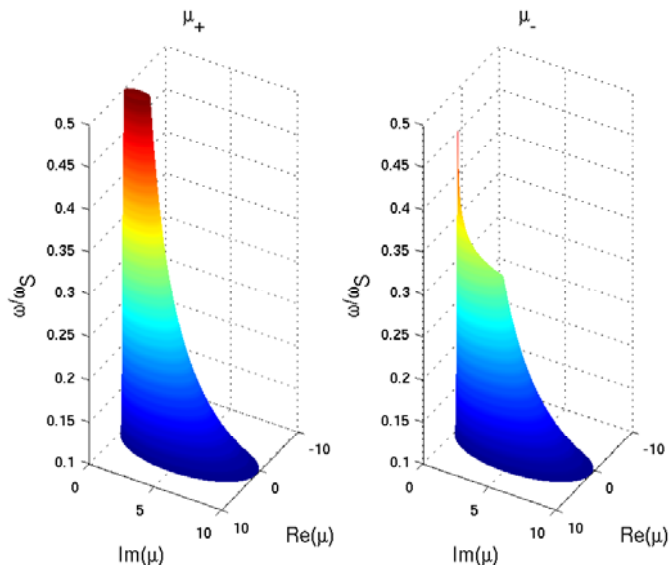
Figure 6: Bounds in the complex plane for the eigenvalues of the susceptibility given in (3.21). The bounds correspond to the dashed curves in Figure 5, using $\mu_1 = \mu_\pm$ according to (6.19) and $\mu_2 = 1$ and volume fraction $f_1 = 0.1$. The bias parameter is $\beta = -0.3$, and the loss factor is $\alpha = 0.1$. The normalized frequency ω/ω_S is along the vertical axis. Left plot shows the bounds for μ_+, and the right plot is for μ_-. Note that only μ_- has a resonance, and is very close to 1 for $\omega/\omega_S > 0.4$.

for a fixed vector $\boldsymbol{H}$. In particular, this applies to the eigenvalues. This region can be calculated by knowledge of only a very limited number of points in the complex plane. When mixing two materials with complex permeabilities μ_1 and μ_2 in volume fractions f_1 and f_2, let z_1 be the arithmetic mean $z_1 = f_1\mu_1 + f_2\mu_2$ and z_2 be the harmonic mean $z_2 = 1/(f_1/\mu_1 + f_2/\mu_2)$. Further, let z_3 be given by (6.1) and z_4 be given by (6.1) but with the roles of materials 1 and 2 interchanged. Let $\mathrm{Arc}(w_1, w_2, w_3)$ denote the circular arc starting in w_1 and ending in w_2, such that when extended it passes through w_3. The effective permeability is then confined in the region between the arcs $\mathrm{Arc}(z_1, z_2, \mu_1)$ and $\mathrm{Arc}(z_1, z_2, \mu_2)$. If it is also known that the effective material is isotropic, a tighter bound is given by the arcs $\mathrm{Arc}(z_3, z_4, z_1)$ and $\mathrm{Arc}(z_3, z_4, z_2)$. An example of these bounds is given in Figure 5.

One problem with these bounds is that they are defined for a fixed frequency, but the susceptibility given in (3.21) depends on frequency. In Figure 6 we have plotted the boundary of the region in the complex plane as a function of frequency along the vertical axis, one plot for each eigenvalue of the susceptibility tensor. In Appendix B and also [25], it is shown that the eigenvalues are

$$\mu_\pm = 1 + \frac{1}{\beta - i\alpha\omega/\omega_S \mp \omega/\omega_S} \tag{6.19}$$

from which it is seen that for a fixed bias parameter only one of the eigenvalues can have a positive resonance frequency. This is seen as an irregular feature in the right

part of the figure, which is not present in the left. It is also seen that the bounds are relatively wide for small frequencies, but sharpen as the frequency becomes higher. This reflects the fact that for higher frequencies, the magnetic properties of the material μ_1 become similar to the surrounding medium $\mu_2 = 1$.

The bounds used in this subsection only rely on knowledge of the volume fraction of the materials. With more knowledge of the microstructure, tighter bounds can be formulated [9, 23].

7 Conclusions

We have used the LLG equation to model the response of a ferromagnetic material to an applied magnetic field. Based on the magnetic properties of a ferromagnetic spherical particle, a small signal model for composite media is developed. It takes into account the resonant behavior and the gyrotropic structure of each particle. This resulted in the composite material also being gyrotropic and resonant.

When comparing the resonance frequency of the single particle and the composite material, respectively, it is important to be consistent in the choice of the input signal. We assert that the appropriate input signal is the field external to the magnetic particles, corresponding to the field inside the composite. This is shown to imply that the resonance frequency of the single particle and the composite material are the same, and specifically the resonance frequency of the composite material does not depend on volume fraction, in contrast to the case for dielectric media [18].

The magnetic losses are characterized in terms of a magnetic conductivity, which can be controlled to some degree by an external, static bias field. The magnetic conductivity is proportional to the saturation magnetization M_S, showing that in order to obtain high losses, materials with high M_S are preferable. Also, for zero bias, the magnetic conductivity is independent of frequency and proportional to the volume fraction.

For small particles, *i.e.*, nanoparticles, some interesting features were found. First, it was shown that at microwave frequencies, eddy currents could be neglected. Secondly, a uniform time harmonic small signal field was shown to be able to excite exchange modes, resulting in additional resonances which add to the loss mechanisms. Surface anisotropy and particle size are important parameters determining these resonance frequencies. Taking these exchange modes into account, a spatially dependent expression for the small signal magnetization in a spherical particle was derived.

Finally, bounds in the complex plane have been presented for the diagonal elements of the effective permeability. The primary use of these bounds is to determine which ranges of complex permeabilities can not be synthesized in a composite material, given knowledge of the constituents.

When deriving our results, we have made some assumptions. The two most important are: 1) All particles must be aligned and have the same shape (spherical). One way of generalizing this may be to use results for polycrystals [23], but it is then very difficult to calculate the static field. 2) Only two component materials

can be used in the composite material, and one material must be isotropic. This is no restriction for numerical approaches, but limits the possible analytical results.

Appendix A Calculation of the induced magnetic moment

In this appendix we estimate the effect of eddy currents in a small particle. Ignoring the skin effect there is no coupling to the induced magnetic field, and we can compute the induced electric field from Faraday's law,

$$\nabla \times \boldsymbol{E} = \mathrm{i}\omega \boldsymbol{B} \tag{A.1}$$

Choosing the z-direction so that $\boldsymbol{B} = B\hat{\boldsymbol{z}}$, symmetry requires (where φ is the azimuth angle)

$$\boldsymbol{E} = E(r_\mathrm{c})\hat{\boldsymbol{\varphi}}, \quad r_\mathrm{c} = \sqrt{x^2 + y^2} \tag{A.2}$$

Using the integral form of Faraday's law, we find

$$2\pi r_\mathrm{c} E(r_\mathrm{c}) = \mathrm{i}\omega B \pi (r_\mathrm{c})^2 \quad \Rightarrow \quad E(r_\mathrm{c}) = \frac{\mathrm{i}\omega B}{2} r_\mathrm{c} \tag{A.3}$$

This corresponds to a current density $\boldsymbol{J} = \sigma \boldsymbol{E} = \sigma E(r_\mathrm{c})\hat{\boldsymbol{\varphi}}$, which corresponds to an induced magnetic moment,

$$\boldsymbol{m} = \frac{1}{2} \int_V \boldsymbol{x} \times \boldsymbol{J}(\boldsymbol{x}) \, \mathrm{d}V \tag{A.4}$$

where the integration should be performed over the particle volume. For a spherical particle with radius R, we have

$$\boldsymbol{m} = \frac{1}{2} \int_{r=0}^{R} \int_{\theta=0}^{\pi} \int_{\varphi=0}^{2\pi} r\hat{\boldsymbol{r}} \times \frac{\mathrm{i}\omega\sigma B}{2} \underbrace{r\sin\theta}_{=r_\mathrm{c}} \hat{\boldsymbol{\varphi}} r^2 \sin\theta \, \mathrm{d}r \, \mathrm{d}\theta \, \mathrm{d}\varphi$$

$$= -\frac{\mathrm{i}\omega\sigma B}{4} \int_{r=0}^{R} \int_{\theta=0}^{\pi} \int_{\varphi=0}^{2\pi} r^4 \sin^2\theta \hat{\boldsymbol{\theta}} \, \mathrm{d}r \, \mathrm{d}\theta \, \mathrm{d}\varphi \tag{A.5}$$

Since $\int_{\varphi=0}^{2\pi} \hat{\boldsymbol{\theta}} \, \mathrm{d}\varphi = -2\pi \sin\theta\hat{\boldsymbol{z}}$, this is

$$\boldsymbol{m} = \frac{\mathrm{i}\omega\sigma B\pi}{2}\hat{\boldsymbol{z}} \int_{r=0}^{R} r^4 \sin^3\theta \, \mathrm{d}r \, \mathrm{d}\theta = \mathrm{i}\omega\sigma B\pi\hat{\boldsymbol{z}} \frac{R^5}{5} \int_{\theta=0}^{\pi} (1 - \cos^2\theta)\sin\theta \, \mathrm{d}\theta$$

$$= \mathrm{i}\omega\sigma B\pi\hat{\boldsymbol{z}} \frac{R^5}{10} \left[-\cos\theta + \frac{\cos^3\theta}{3} \right]_{\theta=0}^{\pi} \hat{\boldsymbol{z}} = \mathrm{i}\omega\sigma B\pi \frac{R^5}{10}(2 - \frac{2}{3})\hat{\boldsymbol{z}}$$

$$= \mathrm{i}\omega\sigma R^5 \frac{2\pi}{15} B\hat{\boldsymbol{z}} \tag{A.6}$$

Thus, we see that the induced magnetic moment from an applied field $\boldsymbol{B}$ is

$$\boldsymbol{m} = \mathrm{i}\omega\sigma R^5 \frac{2\pi}{15} \boldsymbol{B} \tag{A.7}$$

in the limit where the interaction with the field is weak, *i.e.*, the skin depth is large compared to the particle size.

Appendix B Calculation of effective material parameters

In this appendix we give the most important of the calculations leading to the effective material parameters presented in the paper.

B.1 Eigenvectors of the effective permeability

We demonstrate that the effective tensor defined by (6.2) has the same eigenvectors as the original tensor $\boldsymbol{\mu}_1$. Start by multiplying (6.2) with $(\mu_2\mathbf{I} + (f_2/3)(\boldsymbol{\mu}_1 - \mu_2\mathbf{I})$ from the right,

$$\boldsymbol{\mu}_{\mathrm{eff}}[\mu_2\mathbf{I} + (f_2/3)(\boldsymbol{\mu}_1 - \mu_2\mathbf{I})] = \mu_2[\mu_2\mathbf{I} + (f_2/3)(\boldsymbol{\mu}_1 - \mu_2\mathbf{I})] + f_1\mu_2(\boldsymbol{\mu}_1 - \mu_2\mathbf{I}) \quad \text{(B.1)}$$

The tensor in the right hand is a linear combination of identity tensors and $\boldsymbol{\mu}_1$. This means it has the same eigenvectors as $\boldsymbol{\mu}_1$. The same reasoning follows for the tensor in square brackets in the left hand side. Let $\boldsymbol{H}$ be an eigenvector of $\boldsymbol{\mu}_1$. Multiplying both sides with this vector we find

$$\boldsymbol{\mu}_{\mathrm{eff}}\lambda_1\boldsymbol{H} = \lambda_2\boldsymbol{H} \quad \text{(B.2)}$$

where λ_1 and λ_2 are the eigenvalues of the tensors discussed above, being linear combinations of $\mathbf{I}$ and $\boldsymbol{\mu}_1$. This demonstrates that $\boldsymbol{H}$ is also an eigenvector of $\boldsymbol{\mu}_{\mathrm{eff}}$.

Since the effective material has the same set of eigenvectors as $\boldsymbol{\mu}_1$ (but not the same eigenvalues!), the equation (6.2) reduces to the scalar equation (6.1) for the eigenvalues. Thus, we can use (6.1) to get the eigenvalues of the effective tensor. These can later be synthesized together with the eigenvectors to form the final effective tensor.

The eigenvectors in our case are given by the following, where we ignore anisotropy for simplicity. The permeability is given by $\boldsymbol{\mu} = \mathbf{I} + \boldsymbol{\chi}$, where the susceptibility $\boldsymbol{\chi}$ is given by (3.21) and $\beta = |\boldsymbol{H}_0^{\mathrm{e}}|/M_{\mathrm{S}} - 1/3$ for spherical particles. This describes a gyrotropic material, and is usually represented in the form

$$\boldsymbol{\mu} = \begin{pmatrix} \mu & -\mathrm{i}\mu_{\mathrm{g}} & 0 \\ \mathrm{i}\mu_{\mathrm{g}} & \mu & 0 \\ 0 & 0 & 1 \end{pmatrix} \quad \text{(B.3)}$$

It is well known that the eigenvectors of this kind of matrix correspond to circularly polarized waves, $i.e.$,

$$\boldsymbol{H}_{\pm} = \hat{\boldsymbol{x}} \pm \mathrm{i}\hat{\boldsymbol{y}}, \quad \boldsymbol{H}_z = \hat{\boldsymbol{z}} \quad \text{(B.4)}$$

with the corresponding eigenvalues

$$\begin{aligned}
\mu_{\pm} = \mu \pm \mu_{\mathrm{g}} &= 1 + \frac{\beta - \mathrm{i}\alpha\omega/\omega_{\mathrm{S}}}{-(\omega/\omega_{\mathrm{S}})^2 + (\beta - \mathrm{i}\alpha\omega/\omega_{\mathrm{S}})^2} \pm \frac{\omega/\omega_{\mathrm{S}}}{-(\omega/\omega_{\mathrm{S}})^2 + (\beta - \mathrm{i}\alpha\omega/\omega_{\mathrm{S}})^2} \\
&= 1 + \frac{\beta - \mathrm{i}\alpha\omega/\omega_{\mathrm{S}} \pm \omega/\omega_{\mathrm{S}}}{(\beta - \mathrm{i}\alpha\omega/\omega_{\mathrm{S}} + \omega/\omega_{\mathrm{S}})(\beta - \mathrm{i}\alpha\omega/\omega_{\mathrm{S}} - \omega/\omega_{\mathrm{S}})} \\
&= 1 + \frac{1}{\beta - \mathrm{i}\alpha\omega/\omega_{\mathrm{S}} \mp \omega/\omega_{\mathrm{S}}} \quad \text{(B.5)}
\end{aligned}$$

and the trivial eigenvalue $\mu_z = 1$ for the eigenvector $\boldsymbol{H}_z = \hat{\boldsymbol{z}}$.

B.2   Frequency dependence

When studying a mixture of two isotropic dielectric materials, it is shown in [18] that if the permittivity of material 1 can be written

$$\epsilon_1(\omega) = \frac{\sum_m a_m \omega^m}{\sum_n b_n \omega^n}, \quad b_0 = 1 \tag{B.6}$$

and the Hashin-Shtrikman formula (6.1) is used with a non-dispersive background material ϵ_2, the corresponding coefficients for the effective permittivity are given by

$$a_m^{\text{eff}} = \epsilon_2 \frac{(1 + 2f_1)a_m + 2\epsilon_2(1 - f_1)b_m}{(1 - f_1)a_0 + \epsilon_2(2 + f_1)}, \qquad m = 0, 1, 2, \ldots \tag{B.7}$$

$$b_0^{\text{eff}} = 1 \tag{B.8}$$

$$b_m^{\text{eff}} = \frac{(1 - f_1)a_n + \epsilon_2(2 + f_1)b_n}{(1 - f_1)a_0 + \epsilon_2(2 + f_1)}, \qquad n = 1, 2, 3, \ldots \tag{B.9}$$

It was previously shown that the eigenvectors of a gyrotropic matrix such as our permeability $\boldsymbol{\mu}_1$ correspond to left- and right-hand circularly polarized waves, with eigenvalues

$$\mu_{\pm} = 1 + \frac{1}{\beta - \mathrm{i}\alpha\omega/\omega_{\text{S}} \mp \omega/\omega_{\text{S}}} = \frac{\beta - \mathrm{i}\alpha\omega/\omega_{\text{S}} \mp \omega/\omega_{\text{S}} + 1}{\beta - \mathrm{i}\alpha\omega/\omega_{\text{S}} \mp \omega/\omega_{\text{S}}} = \frac{\frac{1+\beta}{\beta} + \frac{-\mathrm{i}\alpha \mp 1}{\beta\omega_{\text{S}}}\omega}{1 + \frac{-\mathrm{i}\alpha \mp 1}{\beta\omega_{\text{S}}}\omega} \tag{B.10}$$

Thus, all coefficients are zero except

$$a_0^{\pm} = \frac{1+\beta}{\beta_0} \qquad\qquad a_1^{\pm} = \frac{-\mathrm{i}\alpha \mp 1}{\beta\omega_{\text{S}}} \tag{B.11}$$

$$b_0^{\pm} = 1 \qquad\qquad b_1^{\pm} = \frac{-\mathrm{i}\alpha \mp 1}{\beta\omega_{\text{S}}} = a_1^{\pm} \tag{B.12}$$

This implies

$$\mu_{\text{eff}}^{\pm} = \frac{a_0^{\text{eff}\pm} + a_1^{\text{eff}\pm}\omega}{1 + b_1^{\text{eff}\pm}\omega} \tag{B.13}$$

with

$$a_0^{\text{eff}\pm} = \mu_2 \frac{(1 + 2f_1)(1 + 1/\beta) + 2\mu_2(1 - f_1)}{(1 - f_1)(1 + 1/\beta) + \mu_2(2 + f_1)} = a_0^{\text{eff}} \tag{B.14}$$

$$a_1^{\text{eff}\pm} = \mu_2 \frac{(1 + 2f_1) + 2\mu_2(1 - f_1)}{(1 - f_1)(1 + 1/\beta) + \mu_2(2 + f_1)} \frac{-\mathrm{i}\alpha \mp 1}{\beta\omega_{\text{S}}} = \frac{-\mathrm{i}\alpha \mp 1}{\beta\omega_a} \tag{B.15}$$

$$b_1^{\text{eff}\pm} = \frac{(1 - f_1) + \mu_2(2 + f_1)}{(1 - f_1)(1 + 1/\beta) + \mu_2(2 + f_1)} \frac{-\mathrm{i}\alpha \mp 1}{\beta\omega_{\text{S}}} = \frac{-\mathrm{i}\alpha \mp 1}{\beta\omega_b} \tag{B.16}$$

where

$$\omega_a = \frac{\omega_{\mathrm{S}}}{\mu_2} \frac{(1 - f_1)(1 + 1/\beta) + \mu_2(2 + f_1)}{(1 + 2f_1) + 2\mu_2(1 - f_1)} \tag{B.17}$$

$$\omega_b = \omega_{\mathrm{S}} \frac{(1 - f_1)(1 + 1/\beta) + \mu_2(2 + f_1)}{(1 - f_1) + \mu_2(2 + f_1)} \tag{B.18}$$

The homogenized tensor is found from the combinations

$$\mu_{\mathrm{eff}}^{+} \pm \mu_{\mathrm{eff}}^{-} = \frac{a_0^{\mathrm{eff}} + \frac{-\mathrm{i}\alpha-1}{\beta\omega_a}\omega}{1 + \frac{-\mathrm{i}\alpha-1}{\beta\omega_b}\omega} \pm \frac{a_0^{\mathrm{eff}} + \frac{-\mathrm{i}\alpha+1}{\beta\omega_a}\omega}{1 + \frac{-\mathrm{i}\alpha+1}{\beta\omega_b}\omega} = \frac{a_0^{\mathrm{eff}} + \frac{-\mathrm{i}\alpha\omega}{\beta\omega_a} - \frac{\omega}{\beta\omega_a}}{1 + \frac{-\mathrm{i}\alpha\omega}{\beta\omega_b} - \frac{\omega}{\beta\omega_b}} \pm \frac{a_0^{\mathrm{eff}} + \frac{-\mathrm{i}\alpha\omega}{\beta\omega_a} + \frac{\omega}{\beta\omega_a}}{1 + \frac{-\mathrm{i}\alpha\omega}{\beta\omega_b} + \frac{\omega}{\beta\omega_b}} \tag{B.19}$$

This is on the form

$$\frac{a - b}{c - d} \pm \frac{a + b}{c + d} = \frac{(a - b)(c + d) \pm (a + b)(c - d)}{(c - d)(c + d)}$$

$$= \frac{ac + ad - bc - bd \pm (ac - ad + bc - bd)}{c^2 - d^2} = \begin{cases} 2\dfrac{ac - bd}{c^2 - d^2} \\[2mm] 2\dfrac{ad - bc}{c^2 - d^2} \end{cases} \tag{B.20}$$

which means we have

$$\mu_{\mathrm{eff}} = \frac{\mu_{\mathrm{eff}}^{+} + \mu_{\mathrm{eff}}^{-}}{2} = \frac{(a_0^{\mathrm{eff}} - \frac{\mathrm{i}\alpha\omega}{\beta\omega_a})(1 - \frac{\mathrm{i}\alpha\omega}{\beta\omega_b}) - \frac{\omega^2}{\beta^2\omega_a\omega_b}}{(1 - \frac{\mathrm{i}\alpha\omega}{\beta\omega_b})^2 - \frac{\omega^2}{\beta^2\omega_b^2}}$$

$$= \frac{a_0^{\mathrm{eff}} - \frac{\mathrm{i}\alpha\omega}{\beta\omega_b}\left(a_0^{\mathrm{eff}} + \frac{\omega_b}{\omega_a}\right) - (1 + \alpha^2)\frac{\omega^2}{\beta^2\omega_a\omega_b}}{(1 - \frac{\mathrm{i}\alpha\omega}{\beta\omega_b})^2 - \frac{\omega^2}{\beta^2\omega_b^2}} \tag{B.21}$$

and

$$\mu_{\mathrm{g,eff}} = \frac{\mu_{\mathrm{eff}}^{+} - \mu_{\mathrm{eff}}^{-}}{2} = \frac{(a_0^{\mathrm{eff}} - \frac{\mathrm{i}\alpha\omega}{\beta\omega_a})\frac{\omega}{\beta\omega_b} - (1 - \frac{\mathrm{i}\alpha\omega}{\beta\omega_a})\frac{\omega}{\beta\omega_b}}{(1 - \frac{\mathrm{i}\alpha\omega}{\beta\omega_b})^2 - \frac{\omega^2}{\beta^2\omega_b^2}} = \frac{(a_0^{\mathrm{eff}} - \frac{\omega_b}{\omega_a})\frac{\omega}{\beta\omega_b}}{(1 - \frac{\mathrm{i}\alpha\omega}{\beta\omega_b})^2 - \frac{\omega^2}{\beta^2\omega_b^2}} \tag{B.22}$$

In conclusion, we have

$$\boldsymbol{\mu}_{\mathrm{eff}} = \begin{pmatrix} \mu_{\mathrm{eff}} & -\mathrm{i}\mu_{g,\mathrm{eff}} & 0 \\ \mathrm{i}\mu_{g,\mathrm{eff}} & \mu_{\mathrm{eff}} & 0 \\ 0 & 0 & \mu_{z,\mathrm{eff}} \end{pmatrix} \tag{B.23}$$

where μ_{eff} and $\mu_{\mathrm{g,eff}}$ are given above, and

$$\mu_{z,\mathrm{eff}} = \mu_2 + \frac{3f_1\mu_2(1 - \mu_2)}{3\mu_2 + (1 - f_1)(1 - \mu_2)} \tag{B.24}$$

References

[1] A. Aharoni. Exchange resonance modes in a ferromagnetic sphere. *J. Appl. Phys.*, **69**, 7762–7764, 1991.

[2] A. Aharoni. Effect of surface anisotropy on the exchange resonance modes. *J. Appl. Phys.*, **81**, 830–833, 1997.

[3] A. A. Barybin. Modal expansions and orthogonal complements in the theory of complex media waveguide excitation by external sources for isotropic, anisotropic, and bianisotropic media. *Progress in Electromagnetics Research*, **19**, 241–300, 1998.

[4] A. A. Barybin. Excitation theory for space-dispersive active media and waveguides. *J. Phys. D: Applied Phys.*, **32**, 2014–2028, 1999.

[5] V. B. Bregar. Advantages of ferromagnetic nanoparticle composites in microwave absorbers. *IEEE Trans. Magnetics*, **40**(3), 1679–1684, May 2004.

[6] W. F. Brown. *Micromagnetics*. Interscience Publishers, New York, 1963.

[7] M. d'Aquino. *Nonlinear Magnetization Dynamics in Thin-films and Nanoparticles*. PhD thesis, Universita degli studi di Napoli "Federico II", Facolta di Ingegneria, December 2004.

[8] W. E. Selected problems in materials science. In B. Engquist and W. Schmid, editors, *Mathematics Unlimited — 2001 and Beyond*, pages 407–432. Springer-Verlag, Berlin, 2001.

[9] C. Engström. Bounds on the effective tensor and the structural parameters for anisotropic two-phase composite material. *J. Phys. D: Applied Phys.*, **38**, 3695–3702, 2005.

[10] T. L. Gilbert. A phenomenological theory of damping in ferromagnetic materials. *IEEE Trans. Magnetics*, **40**(6), 3443–3449, November 2004.

[11] J. B. Goodenough. Summary of losses in magnetic materials. *IEEE Trans. Magnetics*, **38**(5), 3398–3408, September 2002.

[12] J. D. Jackson. *Classical Electrodynamics*. John Wiley & Sons, New York, third edition, 1999.

[13] D. M. Johannsen, U. Gneveckow, L. Eckelt, A. Feussner, N. Waldöfner, R. Scholz, S. Deger, P. Wust, S. A. Loening, and A. Jordan. Clinical hyperthermia of prostate cancer using magnetic nanoparticles: Presentation of a new interstitial technique. *International Journal of Hyperthermia*, **21**(7), 637–647, November 2005.

[14] C. Kittel. Excitation of spin waves in a ferromagnet by a uniform rf field. *Phys. Rev.*, **110**(6), 1295–1297, June 1958.

[15] C. Kittel. On the theory of ferromagnetic resonance absorption. *Phys. Rev.*, **73**(2), 155–161, 1948.

[16] C. Kittel. *Introduction to Solid State Physics.* John Wiley & Sons, New York, 7 edition, 1996.

[17] E. F. Knott, J. F. Shaeffer, and M. T. Tuley. *Radar Cross Section.* SciTech Publishing Inc., 5601 N. Hawthorne Way, Raleigh, NC 27613, 2004.

[18] G. Kristensson, S. Rikte, and A. Sihvola. Mixing formulas in the time domain. *J. Opt. Soc. Am. A*, **15**(5), 1411–1422, May 1998.

[19] L. D. Landau and E. M. Lifshitz. On the theory of the dispersion of magnetic permeability in ferromagnetic bodies. *Physik. Z. Sowjetunion*, **8**, 153–169, 1935. Reprinted by Gordon and Breach, Science Publishers, "Collected Papers of L. D. Landau", D. Ter Haar, editor, 1965, pp. 101–114.

[20] L. D. Landau, E. M. Lifshitz, and L. P. Pitaevskiĭ. *Electrodynamics of Continuous Media.* Pergamon, Oxford, second edition, 1984.

[21] D. Mercier, J. S. Lévy, G. Viau, F. Fiévet-Vincent, F. Fiévet, P. Toneguzzo, and O. Acher. Magnetic resonance in spherical Co-Ni and Fe-Co-Ni particles. *Phys. Rev. B*, **62**(1), 532–544, 2000.

[22] G. W. Milton. Bounds on the complex dielectric constant of a composite material. *Appl. Phys. Lett.*, **37**(3), 300–302, 1980.

[23] G. W. Milton. *The Theory of Composites.* Cambridge University Press, Cambridge, U.K., 2002.

[24] K. Raj and R. Moskowitz. Commercial applications of ferrofluids. *J. Magn. Magn. Mater.*, **85**, 233–245, 1990.

[25] J. Ramprecht and D. Sjöberg. Biased magnetic materials in RAM applications. *Progress in Electromagnetics Research*, **75**, 85–117, 2007.

[26] A. Sihvola. *Electromagnetic Mixing Formulae and Applications.* IEE Electromagnetic Waves Series, 47. Institution of Electrical Engineers, 1999.

[27] D. Sjöberg. Circuit analogs for stratified structures. Technical Report LUTEDX/(TEAT-7159)/1–18/(2007), Lund University, Department of Electrical and Information Technology, P.O. Box 118, S-221 00 Lund, Sweden, 2007. http://www.eit.lth.se.

[28] P. Toneguzzo, G. Viau, O. Archer, F. Guillet, E. Bruneton, F. Fiévet-Vincent, and F. Fiévet. CoNi and FeCoNi fine particles prepared by the polyol process: Physico-chemical characterization and dynamic magnetic properties. *Journal of Material Science*, **35**, 3767–3784, 2000.

[29] G. Viau, F. Fiévet, P. Toneguzzo, F. Ravel, and O. Acher. Size dependence of microwave permeability of spherical ferromagnetic particles. *J. Appl. Phys.*, **81**(6), 2749–2754, 1997.

[30] P. A. Voltairas, D. Fotiadis, and C. V. Massalas. Mode mixing in ferromagnetic resonance in magnetic microspheres. *J. Appl. Phys.*, **88**(1), 374–378, July 2000.

[31] L. Z. Wu, J. Ding, H. B. Jiang, L. F. Chen, and C. K. Ong. Particle size influence to the microwave properties of iron based magnetic particulate composites. *J. Magn. Magn. Mater.*, **285**, 233–239, 2005.

[32] Y. Yu and J. W. Harrell. FMR spectra of oriented γ-Fe$_2$O$_3$, Co-γ-Fe$_2$O$_3$, CrO$_2$ and MP tapes. *IEEE Trans. Magnetics*, **30**(6), 4083–4085, November 1994.